Published in final edited form as:
*Methods Cell Biol*. 2011 ; 103: 115–147. doi:10.1016/B978-0-12-385493-3.00006-1.

# Analysis of Individual Molecular Events of DNA Damage Response by Flow and Image Assisted Cytometry

**Zbigniew Darzynkiewicz**[1], **Frank Traganos**[1], **Hong Zhao**[1], **H. Dorota Halicka**[1], **Joanna Skommer**[2], and **Donald Wlodkowic**[3]

[1]Brander Cancer Research Institute and Department of Pathology, New York Medical College, Valhalla, NY, USA [2]School of Biological Sciences, University of Auckland, Auckland, New Zealand [3]Auckland Microfabrication Facility, Department of Chemistry, University of Auckland, Auckland, New Zealand

## Abstract

This chapter describes molecular mechanisms of DNA damage response (DDR) and presents flow- and image-assisted cytometric approaches to assess these mechanisms and measure the extent of DDR in individual cells. DNA damage was induced by cell treatment with oxidizing agents, UV light, DNA topoisomerase I or II inhibitors, cisplatin, tobacco smoke, and by exogenous and endogenous oxidants. Chromatin relaxation (decondensation) is an early event of DDR chromatin that involves modification of high mobility group proteins (HMGs) and histone H1 and was detected by cytometry by analysis of the susceptibility of DNA *in situ* to denaturation using the metachromatic fluorochrome acridine orange. Translocation of the MRN complex consisting of Meiotic Recombination 11 Homolog A (Mre11), Rad50 homolog and Nijmegen Breakage Syndrome 1 (NMR1) into DNA damage sites was assessed by laser scanning cytometry as the increase in the intensity of maximal pixel as well as integral value of Mre11 immunofluorescence. Examples of cytometric detection of activation of *Ataxia telangiectasia mutated* (ATM), and Check 2 (Chk2) protein kinases using phospho-specific Abs targeting Ser1981 and Thr68 of these proteins, respectively are also presented. We also discuss approaches to correlate activation of ATM and Chk2 with phosphorylation of p53 on Ser15 and histone H2AX on Ser139 as well as with cell cycle position and DNA replication. The capability of laser scanning cytometry to quantify individual foci of phosphorylated H2AX and/or ATM that provides more dependable assessment of the presence of DNA double-strand breaks is outlined. The new microfluidic Lab-on-a-Chip platforms for interrogation of individual cells offer a novel approach for DDR cytometric analysis.

## II. Introduction

Intricate and highly choreographed series of molecular events broadly defined as the DNA damage response (DDR) take place in the live cell upon induction of DNA damage. The events of DDR involve a multitude of post-translational modifications of proteins that trigger interactions between intracellular molecules activating several signaling pathways. Pathway activation has four critical aims: (i) stopping cell cycle progression and division and thereby preventing transfer of damaged DNA to progeny cells; (ii) enhancing accessibility of the damage site to the DNA repair machinery; (iii) activating and engaging repair machinery, and (iv) triggering apoptosis or inducing cellular senescence (reproductive

*Corresponding author:* Dr. Z. Darzynkiewicz, Brander Cancer Research Institute at NYMC, Department of Pathology, BSB 438, Valhalla, NY 10595, Tel: 914-594-3780, Fax: 914-594-3790, darzynk@nymc.edu.

cell death) to eliminate cells whose damaged DNA cannot successfully be repaired (reviews, Bakkenist and Kastan, 2003, 2004; Bonner *et al.*, 2008; Helt *et al.*, 2005; Kastan, 2008; Lee and Paull, 2005, Nakamura *et al.*, 2010). This review briefly describes the molecular mechanisms of DDR and outlines applications of cytometry in analysis of particular events and stages of DDR.

## III. Events of the DDR

### A. Chromatin decondensation (relaxation)

One of the early events of the DDR is remodeling of chromatin structure that involves its decondensation (Murga *et al.*, 2007; Pandita and Richardson, 2009; Rouleau *et al.*, 2004; Ziv *et al.*, 2006). Chromatin decondensation appears to be triggered by decline of torsional strain of the DNA double helix occurring upon DNA damage, particularly when the damage involves formation of DNA double-strand breaks (DSBs) (Fig. 1). DNA torsional strain (topological stress) is otherwise maintained by its winding onto histone octamers of the nucleosome core and supercoiling to form the supra-nucleosomal chromatin structure (Marko, 2010). High mobility group proteins (HMGs) play a key role in providing a rapid dynamic response by local decondensation of chromatin triggered by DNA damage (Gerlitz and Bustin, 2009, Kim *et al.*, 2009, Sinha and Peterson, 2009). HMGs and histone H1 are persistently moving along the chromatin fiber and interacting with each other and with internucleosomal DNA. Compared with other nuclear proteins, HMGs are the most extensively modified, being rapidly phosphorylated, acetylated, methylated, ribosylated and/or sumoylated in response to changes in the physiological state of the cell, induction of stress or cell cycle phase (Zhang and Wang, 2008). This network provides a continuous highly dynamic interplay between a variety of nuclear structural proteins, modulating their binding to each other and to nucleosomes (Lim *et al.*, 2004; Misteli and Soutoglou, 2009). Of particular importance is the binding of the HMGN1 protein to the nucleosome, which alters the architecture of chromatin and affects the levels of post-transcriptional modifications of the tails of nucleosomal histones. Specifically, upon HMGN1 binding to nucleosomes, phosphorylation of histone H3 on Ser10 is reduced (Lim *et al.*, 2004). Since histone H3 phosphorylation on Ser10 is required to maintain chromatin in a condensed state such as during mitosis (Juan *et al.*, 1998) or premature chromosome condensation (Huang *et al.*, 2006a) the reduction of its level of phosphorylation facilitates chromatin decondensation (relaxation). Thus, the DNA damage-induced activation of HMGN1 and its binding to nucleosomes preventing histone H3 phosphorylation may directly mediate chromatin decondensation.

Histone acetyltransferase TIP60 also plays a role in modulation of chromatin dynamics. After damage to DNA, in addition to acetylation of histone H2AX, which is a prerequisite for its phosphorylation on Ser139, TIP60 regulates the ubiquitination of H2AX via the ubiquitin-conjugating enzyme UBC (Ikura *et al.*, 2007, Kruhlak *et al.*, 2006). Sequential acetylation and ubiquitination of H2AX by TIP60-UBC promotes enhanced histone dynamics, which in turn stimulates the DDR. It should be noted that the presence of wt p53 appears to be critical for the induction of chromatin relaxation upon DNA damage (Murga *et al.*, 2007, Rubi and Milner, 2003) perhaps through its effect on the tumor suppressor p33ING2 (Wang *et al.*, 2006). Chromatin relaxation augments accessibility of the repair machinery to DNA damage sites and appears to also provide the signal for activation of *Ataxia Telangiectasia Mutated* (ATM) protein kinase.

The MRN complex consisting of Meiotic Recombination 11 Homolog A (Mre11), Rad50 homolog and Nijmegen Breakage Syndrome 1 (NMR1) proteins undergoes translocation into the site of DNA damage at the time of chromatin decondensation and activation of the ATM protein kinase (Abraham and Tibbetts, 2005; Downs and Cote, Kitagawa and Kastan,

2005, 2005; Paull and Lee, 2005). It should be noted that ATM activation takes place at some distance from the DNA break site and the activated kinase moves then to the site.

### B. Activation of phosphatidyl inositol 3' kinase-related kinases (PIKKs)

The DDR is regulated by three PIKKs: ATM, ATM and Rad3-related (ATR), and DNA dependent protein kinase (DNA-PKcs) (Cuadrado *et al.*, 2006, Helt *et al.*, 2005, Hill and Lee, 2010, Lovejoy and Cortez, 2009). These kinases are primarily responsible for signaling the presence of DNA damage and phosphorylate hundreds of proteins whose function is to maintain the integrity of the genome. The substrates phosphorylated by these PIKKs are implicated in regulation of DNA damage repair, cell cycle progression, apoptosis and cell senescene. In many instances these PIKKs can have redundant activities and back-up each other in terms of phosphorylation of the same proteins.

Among the PIKKs that are activated in response to DNA damage the most extensively studied was ATM, which is the key component of the signal transduction pathways mobilized by the induction of DSBs (Li and Zou, 2005; Shiloh, 2003). Activation of ATM occurs through its autophosphorylation on *Ser*1981 and requires its prior acetylation which is mediated by the Tip60 histone acetyltransferase (Sun *et al.*, 2005). ATM phosphorylation leads to dissociation of the inactive ATM dimers onto monomers that have kinase catalytic activity (Bakkenist and Kastan, 2003, 2004) (Fig. 1). The MRN protein complex plays a critical role in the process of ATM activation as it detects DNA damage, recruits ATM to the damage site and targets ATM to the respective substrates to initiate their phosphorylation (Lee and Paull, 2005). Whereas ATM phosphorylation on *Ser*1981 is a prerequisite for dissociation of the dimer, the catalytic domain of ATM is outside of the *Ser*1981 site and becomes accessible to the kinase substrates only when ATM is in its monomeric conformation (Bakkenist and Kastan, 2004).

As schematically presented in Fig. 1 ATM phosphorylates several substrates at the site of the DSB, including NBS1, Structural Maintenance of Chromosomes 1 (SMC1) and Breast Cancer 1 (BRCA1) proteins. Phosphorylated NBS1 targets ATM towards Chk1, phosphorylated SMC1 engages the S-phase checkpoints halting DNA replication (Kitagawa *et al.*, 2004;Wakeman *et al.*, 2004) and BRCA1 phosphorylation is required to activate this protein along the DNA repair pathway. The BRCA1 (E3-ubiquitin ligase) is involved in several biochemical processes related to DNA repair (Kastan, 2008,Kitagawa and Kastan, 2005). BRCA2 is essential for locating Rad51 to the sites of DNA damage and both BRCA proteins are involved in DNA repair by homologous recombination (HR) (Yuan *et al.*, 1999). The mediator of DNA damage checkpoint 1 (MDC1) is also recruited to the DSB site (Stucki and Jackson, 2004). This nuclear protein activates the S phase- and $G_2$/M phase- cell cycle checkpoints and interacts with phosphorylated histone H2AX near sites of DSB facilitating recruitment of the ATM and other repair factors to the damage foci.

Other than ATM, PIKKs activated in response to DNA damage are ATR and DNA-PKcs (Cuadrado *et al.*, 2006, Helt *et al.*, 2005, Hill and Lee, 2010, Lovejoy and Cortez, 2009). Activation of ATR occurs in response to replication stress (Kurose *et al.*, 2006; Ward *et al.*, 2004) rather than to direct induction of DSBs such as caused by ionizing radiation which triggers activation of ATM. However, activation of DNA-PKcs takes place during repair of DSBs where it is an essential factor for the non-homologous end-joining (NHEJ) mechanism of DNA repair (Hill and Lee, 2010, Smith and Jackson, 1999). Because the NHEJ mechanism also operates during V(D)J recombination and is responsible for antibody diversity (Smith, 2004) DNA-PKcs is a critical element for normal immune development. DNA-PKcs is also strongly implicated in telomere maintenance (Samper *et al.*, 2000). The process of activation and inactivation of DNA-PKcs is mediated by its extensive post-translational modification (Hill and Lee, 2010). Among several sites of its phosphorylation

Thr2609, which becomes autophosphorylated in response to DNA damage by ionizing radiation, has been the most studied (Chan *et al.*, 2002).

### C. Activation of checkpoint kinases

The mosdt important downstream target substrates phosphorylated by PIKKs include p53 (TP53), checkpoint kinase 2 (Chk2) and histone H2AX (Bakkenist and Kastan, 2004; Wakeman *et al.*, 2004). The main purpose of checkpoint pathways activation is to halt progression though the cell cycle until integrity to DNA is restored by the repair mechanisms (Ahn *et al.*, 2002, Matsuoka *et al.*, 2000, Zhou and Elledge, 2000). Chk 2 plays a key role in response of the cell cycle progression machinery to DNA damage. Upon induction of DSBs ATM activates Chk2 by phosphorylating Thr68 of this protein (Fig. 2). This leads to dimerization of Chk2 and acquirement of the kinase catalytic activity (Ahn *et al.*, 2000; Ahn et al, 2002). It should be noted that phosphorylation of Chk2 on Thr68 may also be mediated by ATR; this occurs however in response to replication stress (Matsuoka *et al.*, 2000). Intermolecular phosphorylation on Thr383, Thr387 and Ser516 takes place within the Chk dimers which leads to dissociation of the dimers. Both the monomers and the multiphosphorylated dimers are enzymatically active (Fig. 2). The DNA damage-activated Chk2 undergoes dissociation from chromatin which facilitates further signal amplification and translocation to soluble substrates (Li and Stern, 2005).The enzymatically active monomers as well as dimers of Chk2 phosphorylate numerous downstream substrates including Cdc25A and Cdc25C phosphatases which upon activation induce cell arrest at the $G_1$ or at the transition from $G_2$ to M, respectively (Fig. 2). In addition to cell cycle arrest Chk2 plays a role in mediating the response to DNA damage by promoting apoptosis. For example after DNA damage induced by topo2 inhibitor etoposide, Chk2 phosphorylates and activates the E2F-1 transcription factor that activates apoptotic pathways (Stevens *et al.*, 2003). Likewise, phosphorylation of p53 by Chk2 may lead to upregulation of Bax, an event promoting apoptosis. However, phosphorylation of p53 may also lead to upregulation of $p21^{Waf1}$ providing an additional means to halt cell progression through $G_1$ (Lin *et al.*, 1996). BRCA1 and Promyelocytic Leukemia (PML) proteins may be phosphorylated by Chk2 as well (Lee *et al.*, 2000; Yang *et al.*, 2002). Phosphorylation of BRCA1 engages this protein in the DNA repair pathway whereas phosphorylation of PML increases cells proclivity to undergo apoptosis (Ahn *et al.*, 2004). Activated Chk2 also stabilizes the FoxM1 transcription factor thereby enhancing expression of DNA repair genes (Tan *et al.*, 2007). There is strong redundancy between Chk1 and Chk2 as well as among all three isoforms of Cdc25 (Cdc25A, Cdc25B and Cdc25C) (Boutros *et al*, 2006; 2007, Rudolph, 2007) in their enzymatic activities of phosphorylation (Chk1, Chk2) or dephosphorylation (Cdc25A, Cdc25B, Cdc25C), respectively.

### D. Histone H2AX phosphorylation

Histone H2AX, one of the variants of histone H2A (Thatcher and Gorovsky, 1994), is one of the critical proteins responsible for surveillance of genome integrity (Bassing *et al.*, 2003, Celeste *et al*., 2003;). In response to DNA damage, particularly when the damage involves induction of DSBs, H2AX becomes phosphorylated on *Ser*139 (Rogakou *et al.*, 1998; Sedelnikova *et al.*, 2002). The phosphorylation can be mediated by ATM- (Anderson *et al.* 2001; Burma *et al.*, 2001), ATR- (Furuta *et al.* 2003), and/or DNA-PKcs (Park *et al*,. 2003) and takes place on nucleosomes on both sides flanking DSBs along a megabase domain of DNA (Rogakou *et al.* 1999). The *Ser*-139-phosphorylated H2AX is defined as γH2AX. Of notice, H2AX is also phosphorylated during induction of DSBs in physiological processes such as DNA recombination in V(D)J class-switch during the process of immune system development and in meiosis (Modesti & Kanaar, 2001; Smith, 2004). DNA fragmentation in cells undergoing apoptosis also induces extensive H2AX phosphorylation (Huang *et al.* 2003; Huang *et al.*, 2004; Huang *et al.*, 2005).

## IV. Detection of DDR events by cytometry

### A. Chromatin relaxation (decondensation)

We have recently reported that the DNA damage-induced chromatin decondensation can be detected and measured by flow cytometry (Halicka *et al.*, 2009b). The method is based on the use of the metachromatic fluorochrome acridine orange (AO) which differentially stains double-stranded (ds) versus single-stranded (ss) nucleic acids (Darzynkiewicz *et al.*, 1975). Specifically, AO intercalates between the base pairs of the ds DNA and as a monomer fluoresces green (530 nm). However, when AO binds to ss nucleic acid sections it causes their condensation (transition of the AO-ssDNA complex to solid state) which manifests as red luminescence (>640 nm) that occurs as a result of intersystem crossing (triplet excitation) (Kapuscinski and Darzynkiewicz, 1984a, b). The lifetime of the green fluorescence is ≤3 nsec while the lifetime of the red luminescence is about 9 nsec. The susceptibility of DNA to denaturation when stressed by heat or acid varies with the degree of chromatin condensation and the most susceptible is DNA in highly condensed chromatin of mitotic and apoptotic cells (Dobrucki and Darzynkiewicz, 2001). This propensity of AO to differentially stain DNA in condensed versus decondensed chromatin, assessed by cytometry, has been described by us in different cell systems including spermatogenesis, differentiation, $G_0$ to $G_1$ or $G_2$ to M transition and during apoptosis. In fact, this application of AO to detect abnormal chromatin condensation during spermatogenesis (Evenson *et al.*, 1980) which resembles apoptotic chromatin condensation (Gorczyca *et al.*, 1993) has become widely recognized male fertility assay, defined as the "sperm chromatin structure assay" (SCSA).

As it is evident in Fig. 3 the treatment of cells with UV led to an increase in intensity of green and a decrease of red emission indicating that DNA in the UV treated cells was more resistant to acid driven denaturation. Thus, this simple approach, based on the use AO, detects chromatin decondensation induced by DNA damage. A similar response was observed in other cell types including human lymphocytes, as well as following oxidative DNA damage by $H_2O_2$ (Halicka *et al.*, 2009). The degree of DNA denaturation is presented as the αt index, which represents the ratio of the mean value of red luminescence intensity of the cell subpopulations (reporting AO-interactions with the denatured, ssDNA) to the mean total (red plus green) intensity of the emission. Of interest is the observation that while chromatin decondensation induced by DNA damage caused by UV was global, occurring more or less equally in all phases of the cell cycle, the subsequent events of DDR induced by UV (activation of ATM and induction of γH2AX) were limited to S-phase cells only (Zhao *et al.*, 2009).

### B. Recruitment of Mre11

As mentioned earlier in this chapter, the recruitment of MRN complex of proteins consisting of Mre11-Rad50-NBS1 to the DNA damage site is one of the earliest events of the DDR. This event is essential for activation of ATM. The MRN complex then targets ATM to initiate phosphorylation of the respective substrates (Fig. 1). We attempted to measure this event by cytometry expecting that the recruitment of these proteins to the damage site will be reflected by the increase in maximal pixel of Mre11 immunofluorescence (IF). This would be analogous to the recruitment of Bax to the mitochondrial membrane when this protein, normally diffusely distributed throughout the cell, becomes translocated and locally concentrated in mitochondria upon induction of apoptosis (Bedner *et al.*, 2000).

Our data presented in Fig. 4 indicate that the recruitment of MRN complex induced by DNA oxidative damage in A549 cells can be detected by cytometry as the increase in intensity of Mre11 IF (Zhao *et al.*, 2008a). However, rather unexpectedly we observed that not only the

intensity of maximal pixel increased but Mre11 IF integrated over the whole nucleus also increased. The latter could indicate that either: (i) Mre11 was synthesized after induction of the damage; (ii) Mre11 was translocated from cytoplasm to the nucleus, or (iii) the accessibility of the Mre11 epitope to the Ab was increased when this protein was recruited to the site of DNA damage. The rapidity of the response (<10 min) makes the possibility of synthesis of new Mre11 rather unlikely. Furthermore Mre11 is generally localized in the nucleus although in exceptional instances (viral infection) can be located in the cytoplasm (Araujo *et al.*, 2005). Most likely, therefore, the observed increase in expression of Mre11 (integral) may reflect a change in its conformation that makes the epitope more accessible to the Ab. The epitope of Mre11 detected by this Ab (31H4, rabbit) is a small peptide domain corresponding to a stretch of amino acids in the vicinity of Lys496 of human Mre11A (Zhao *et al.*, 2008a).

The peak of the Mre11 increase occurred within 10 min of exposure of cells to $H_2O_2$ and it preceded by 20 min the peak of activation of ATM and Chk2 as measured by their phosphorylations on Ser1981 and Thr68, respectively and by 60 min the peak of phosphorylation of histone H2AX on Ser139, all measured by LSC (Zhao *et al.*, 2008a)

As it is evident in Fig. 4, in analogy to chromatin relaxation (Fig. 3) the level of Mre11 recruitment was similar in all phases of the cell cycle. However, the DDR events downstream of Mre11 recruitment (ATM and Chk2 activation and H2AX phosphorylation) were distinctly cell cycle phase specific being maximal in S phase cells (Zhao *et al.*, 2008a). This observation suggests that the cell cycle-phase associate factors appear to modulate activation of the events subsequent to Mre11 recruitment.

### C. Immunocytochemical detection of DDR-associated ATM, DNA-PKcs and Chk2 activation, phosphorylation of p53 and histone H2AX

The development of phospho-specific Abs that detect proteins responding to DNA damage by phosphorylation at specific sites (as shown in Figs. 1 and 2) and their application in flow and image-assisted cytometry opened a vast area of experimentation in several directions. Using these Abs it is possible to detect activation of ATM (ATM-S1981$^P$), Chk2 (Chk2-Thr68$^P$) and DNA-PKcs (DNA-PKcsThr2609$^P$) and phoshorylation ofH2AX (γH2AX), as well as p53-Ser15$^P$). All these proteins are the players in the process of DDR. One direction of their use was in the basic research designed to investigate the mechanisms of DDR, especially the relationship of particular events of DDR vis-à-vis cell cycle progression, induction of apoptosis or cell senescence. Another direction was to reveal mechanisms of action of antitumor agents targeting DNA such as DNA topoisomerase I (topo1) and II (topo2) inhibitors, alkylating agents, ionizing and UV radiation. Still another direction was to use this approach to detect and characterize the genotoxicity of a variety of endogenous and exogenous agents. Because the detection of DNA damage by this approach is much more sensitive than by the prior methods (e.g. comets assays) it was possible to detect minute effects including the level of constitutive DNA damage induced by endogenous oxidants in untreated cells, healthy cells. Also, the cytometric assessment of DDR has been proposed and tested as a biomarker of severity of DNA damage and as potentially prognostic reporter of the *in vitro* or *in vivo* effectiveness of cytotoxic drugs. Since the appearance of the first publications on the detection of DDR events by cytometry (Banath and Olive, 2003,Huang *et al.*, 2003) significant progress has been made in all these directions (reviews, Olive, 2005,Tanaka *et al.*, 2006,2007,Zhao *et al.*, 2007). The examples of application of cytometry along these lines are described below and listed in Figs. 5–10.

## V. Application of cytometry to detect DDR induced by different genotoxic agents

### A. Assessment of DDR induced by DNA topoisomerase inhibitors

In one set of experiments we explored the mechanisms of the DDR in A549 cells treated with topo1 (topotecan) and topo2 (mitoxantrone and etoposide) inhibitors in relation to the cell cycle phase and induction of apoptosis (Huang *et al.*, 2003, 2004, 2006b, Kurose *et al.*, 2005, Zhao *et al*, 2008b, 2008c). Topotecan (Tpt), the analog of camptothecin and irinotecan, binds in live cells to DNA-topo1 complexes stabilizing these otherwise cleavable complexes. Collisions between moving replication forks or RNA polymerase molecules and these complexes transform the latter into DSBs resulting in potentially lethal lesions. Topo2 inhibitors were thought to kill cells by a similar mechanism (D'Arpa *et al.*, 1990, Liu *et al.*, 1989). However, by studying the DDR induced by these inhibitors, we observed significant differences between the two types of inhibitors. The data indicate that the mechanism of induction of DNA damage and subsequent apoptosis is very much different for Tpt, versus mitoxantrone (Mxt) versus etoposide.

Figure 5 exemplifies the analysis of kinetics of DDR induced in A549 cells by Tpt, revealed as an activation of ATM (through its phosphorylation on Ser1981) and of Chk2 (through phosphorylation on Thr68) and phosphorylation of p53 on Ser15 (Zhao *et al.*, 2008b). It is quite apparent from these data that the S-phase cells were much more affected by Tpt than $G_1$ or $G_2$M cells. At the peak of response, nearly all S-phase cells had IF above the maximal level of the constitutive expression of ATM-Ser1981$^P$, Chk2-Thr68$^P$ or p53-Ser15$^P$ found in untreated cells (0 time; marked by the respective skewed dashed lines on these distributions). It is also apparent that the kinetics of the induction of ATM-Ser1981$^P$ was different than that of Chk2-Thr68$^P$ and p53-S15$^P$. Whereas the peak of the expression of activated ATM was seen after 1 h of treatment with Tpt the maximal induction of Chk2-Thr68$^P$ and p53-Ser15$^P$ was after 4–6 h of treatment. The cell cycle arrest induced by TPT was revealed as an accumulation of cells in early S phase after 6 h of treatment (see the arrow on the DNA histogram). In parallel to the experiment with Tpt shown in Fig. 5, we studied the DDR kinetics of A549 cells treated with Mxt. The data revealed an entirely different pattern of DDR compared to that induced by Tpt. Specifically, unlike in the case of Tpt, phosphorylation of ATM, Chk2 and p53 triggered by Mxt was more pronounced in $G_1$- rather than in S-phase cells, and the kinetics of phosphorylation of these proteins was also different (Zhao *et al.*, 2008b).

Fig. 6 illustrates an approach to correlate the Tpt induced activation of ATM with phoshorylation of histone H2AX (Tanaka *et al.*, 2006d,2007a). This was achieved by labeling γH2AX and ATM-S1981$^P$ with different color fluorochromes followed by a multivariate "*paint-a-gate*" analysis. The data clearly indicate that the cells in which H2AX become phosphorylated upon treatment with Tpt also have activated ATM. Furthermore, a distinct correlation in the degree of H2AX phosphorylation (intensity of γH2AX IF) and the degree of ATM activation (ATM-S1981$^P$ IF) is apparent. Thus, the data strongly suggest that phosphorylation of H2AX was mediated by ATM (Tanaka *et al.*, 2006d,2007a).

In several studies on the mechanism of induction of DDR and subsequent cell death (apoptosis) induced by topo1 and topo2 inhibitors it was possible to reveal further differences between these inhibitors (Huang *et al.*, 2003, 2004, 2006b, Kurose *et al.*, 2005, Zhao *et al*, 2008b, 2008c). In the case of the topo1 inhibitor Tpt, the mechanism of cell death induction was rather straightforward and can be explained solely by the mechanism proposed by D'Arpa *et al.*, (1990) and Liu *et al.*, (1989) in which stabilization of the topo1-Tpt complex is followed by collision (stalling) of DNA replication forks upon encountering

these complexes, leading to DSBs formation. The Tpt-induced apoptosis was highly selective to DNA replicating cells and no evidence of Tpt-induced DDR among the cells in $G_1$ or $G_2$M phase of the cell cycle was apparent. Also there was no involvement of reactive oxidative species (ROS) in this mode of cell death induced by Tpt (Huang *et al*, 2003, 2004).

In the case of topo2 inhibitor Mxt, all events of the DDR, namely strong activation of ATM and Chk2, and subsequent phosphorylation of p53, and histone H2AX were seen in all phases of the cell cycle. In fact, the intensity of the DDR was much more pronounced in $G_1$ than in S phase of the cycle. Furthermore, a strong involvement of ROS was evident since most of these events were strongly attenuated when the treatment with Mxt was combined with exposure of cells to the ROS scavenger N-acetyl-L-cysteine (NAC; Huang *et al.*, 2006b). Interestingly, despite the fact that $G_1$ cells were most affected by Mxt in terms of induction of DDR, the apoptosis occurring subsequent to treatment was selective to S-phase cells. This observation implied that regardless of the degree of DNA damage, only the damage in the cells replicating DNA but not in $G_1$ or $G_2$M phase cells was effective in triggering apoptosis (Huang *et al.*, 2006b). In this case the collision of replication forks with the primary lesions, whether representing stabilized Mxt-topo2 complexes or ROS-induced oxidative damage, led to their stalling and formation of DSBs, which was the lethal signal triggering apoptosis.

Interestingly, etoposide (VP-16), which like Mxt is also a topo2 inhibitor, induced maximal expression of DDR in $G_1$ cells. Also, as in the case of Mxt, the DDR induced by etoposide was to a large extent attenuated by scavenging ROS with NAC. However, unlike Mxt, etoposide induced apoptosis not exclusively in S in but in other phases of the cycle as well, particularly affecting $G_1$ cells (Tanaka *et al*, 2007c). It should be noted that Mxt belongs to the anthraquinone family of topo2 inhibitors and binds directly to DNA by intercalation (Kapuscinski and Darzynkiewicz, 1986), while etoposide is a member of the podophyllotoxin family, does not bind to DNA but binds stoichiometrically to topo2 (Kingma *et al.*, 1999).These results implied that in addition to the generally accepted mechanism involving collision of replication forks with the “cleavable complexes” (Liu *et al.*, 1989) other mechanisms, different for etoposide as compared to Mxt, contribute to formation of DSBs and to the triggering of apoptosis. This information is of particular importance when a combination of drugs, including Mxt and etoposide, is being considered for cancer treatment.

Since topo2 inhibitors are widely used in oncology, particularly to treat leukemias, we explored the feasibility of assessing the DDR as a potential biomarker predicting clinical outcome during treatment of human leukemias (Halicka *et al.*, 2009a). Towards this end, activation of ATM and phosphorylation of H2AX in leukemic blast cells from the blood of twenty patients diagnosed with acute leukemias and treated with topo2 inhibitors doxorubicin, daunomycin, Mxt or idarubicin was measured. The blood was collected one hour after completion of the drug infusion and the level of phosphorylation of these proteins was compared by flow cytometry to the pre-treatment level of the same patient. The population of blast cells was identified as CD45-dim and by subsequent gating the analysis of expression of ATM-S1981$^P$ and γH2AX was restricted to this population. The post-infusion increase in the extent of ATM activation and H2AX phosphorylation was observed in all twenty patients and a modest correlation between the induction of ATM activation and H2AX phosphorylation in blasts of individual patients was observed. While the number of the studied patients studied (20) and the number of those not responding to treatment (2) was inadequate to conclude whether the assessment of DDR can be clinically prognostic, the findings demonstrated the feasibility of assessment of DDR during the treatment of leukemias with drugs damaging DNA (Halicka *et al.*, 2009a).

### B. Induction of DDR by ionizing radiation and UV light

Peggy Olive and her collaborators pioneered the use of flow cytometry to detect and measure histone H2AX phosphorylation in response to DNA damage caused by ionizing radiation and also by some anticancer drugs including etoposide and cisplatin (Banath and Olive, 2003, Banath *et al.*, 2004, MacPhail *et al.*, 2003a, 2003b, Olive, 2004, Olive and Banath, 2005, 2009, Olive *et al.*, 2004). In the early studies the authors used flow cytometry to correlate the induction of γH2AX by ionizing radiation with cell cycle phase. In several studies they observed a strong correlation between the dose of radiation and intensity of the induced γH2AX IF. The induction of γH2AX 60 min after irradiation was detected with as low as a 20 cGy dose of X-rays (McPhail *et al.*, 2003b). The half-times of the radiation-induced γH2AX IF ranged from 1.6 to 7.2 h, were correlated with a rate of decrease in the number of IF foci and also correlated with clonogenic survival for 10 cell lines (Banath *et al.*, 2004). Also strongly correlated with cell death, assessed by clonogenicity, was expression of γH2AX IF measured 60 min after treatment of Chinese hamster V79 cells with several radiomimetic drugs examined in a range of over two decades of cell kill (Banath and Olive, 2003). This strong relationship between the induction of γH2AX expression and loss of clonogenicity led the authors to postulate that the assessment of H2AX phosphorylation by flow cytometry can be used as a surrogate of the estimate of cell kill (Banath and Olive, 2003). In another study of several human cervical cancer lines, these authors observed that the cell line-dependent differences in the rate of disappearance of X-irradiation induced γH2AX IF were associated with the status of p53 (wt *vs* p53 deficient) and also related in part to intrinsic radiosensitivity of the lines (Banath *et al.*, 2004). In the case of treatment of human and rodent DNA-repair proficient and deficient cell lines with cisplatin, the authors observed that while the initial intensity of H2AX phosphorylation was not of much relevance, the level of the retention of γH2AX foci 24 h after treatment was highly correlated with the fraction of cells that lost their clonogenic potential (Olive and Banath, 2009).

Phosphorylation of H2AX induced by UV is primarily mediated by ATR (Hanasoge and Ljungman, 2007). However, activation of ATM and DNA PKcs in UV treated cells can be redundant to activation of ATR, occur concurrently and may contribute to phosphorylation of H2AX and other downstream protein substrates (Yajima *et al.*, 2009). As many as 570 sites phosphorylated on 464 proteins were detected in M059K glioblastoma cells in response to UV-irradiation (Stokes *et al.*, 2007). Using multiparameter cytometry the induction of DDR by UV was seen exclusively in DNA replicating cells (Zhao *et al.*, 2010). Inhibition of DNA replication by the DNA polymerase inhibitor aphidicolin was shown to prevent the induction of H2AX phosphorylation in UV-irradiated cells (Halicka *et al.*, 2005). Fig 7 illustrates strikingly similar pattern of incorporation of the DNA precursor 5'-ethynyl-2-deoxyuridine (EdU) and the induction of γH2AX by UV-B, vis-à-vis the cell cycle phase, in exponentially growing A549 cells. During 60 min of exposure to EdU one can identify cells with *variable degrees of EdU labeling* having DNA content close to that of $G_1$ and $G_2$M phase cell*s* (panel A). These are the cells entering S phase (eS; initiating DNA replication) as well as the cells entering $G_2$ ($eG_2$; terminating DNA replication) being exposed to the precursor while replicating DNA for variable time intervals, between 0–60 min. As is evident in panel B, the incorporation of EdU was dramatically suppressed after exposure to UV. It is also evident that the pattern of γH2AX expression in UV-treated cells (panel C) resembles very much that of the EdU incorporation into UV-untreated cells. These data and other findings led us to postulate that the mechanism of induction of DDR by UV involves stalling of DNA replication forks upon encountering the UV-induced primary DNA lesions (known to be cyclobutane-pyrimidine dimers and 6–4 (T-C) photoproducts; Sinha and Häder, 2002), which likely leads to formation DSBs (Zhao *et al.*, 2010a). The observed suppression of EdU incorporation (Fig. 7) would be consistent with the stalling of DNA

replication forks. Since we were unable to observe DDR in the cells that do not replicate DNA it is rather unlikely that it is induced during the nucleotide excision repair process, which is the primary mechanism of repair of DNA damage induced by UV (Marti *et al.*, 2006).

### C. Induction of DDR by cigarette smoke (CS) and other environmental mutagens

CS is the primary cause of lung cancer and it also contributes to the development of other malignancies. We have recently developed a rapid and sensitive assay to test the genotoxicity of CS utilizing LSC. The assay is based on the detection of DDR revealed as activation of ATM and phosphorylation of H2AX in normal human bronchial epithelial cells and in pulmonary carcinoma A549 cells shortly following their exposure to CS (Albino *et al*., 2004, 2006, 2009, Jorgensen *et al.*, 2010, Tanaka *et al.*, 2007b, Zhao *et al.*, 2009a).

Fig. 8 demonstrates the use of this assay to compare the genotoxic properties of tobacco and nicotine free cigarettes (T&N free) with that of CS from 2R4F cigarette, a standard cigarette developed by the University of Kentucky (Jorgensen *et al.*, 2010). It is quite evident that 20 min exposure of A549 cells to CS from the 2R4F cigarettes induced both, ATM activation as well as H2AX phosphorylation, and that these effects were the most pronounced in S-phase cells. It is also apparent that exposure of cells to whole smoke from T&N free CS induced both ATM activation and H2AX phosphorylation. The effect, however, was less S-phase specific since $G_1$ and $G_2$M cells showed elevated levels of expression of ATM-S1981$^P$ and γH2AX as well. However, when the smoke from T&N free cigarettes was diluted with an air by creating vents (pores) in the cigarette filters, the effect become more S-phase specific, similar to that of whole smoke from 2R4F cigarettes. These data as well as additional tests revealed that the smoke from T&N free cigarettes, which are commercially available as a substitute for tobacco cigarettes (with the aim to curtail smoking), are even more genotoxic than the tobacco containing cigarettes (Jorgensen *at al.*, 2010).

As exemplified by analysis of genotoxicity of CS, cytometric analysis of DDR provides high sensitivity, convenience and rapidity in detecting the genotoxic potential of different agents. Clearly, the sensitivity of detection of the most deleterious DNA lesions such as DSBs is many-fold higher that that provided by the alternative method, the comet assay. One would expect, therefore, wide application of the cytometric-DDR approach in testing environmental genotoxins as well agents promoted as neutralizers of such toxins. In one such application we have observed that DNA damage in live cells caused by the acridine mutagen ICR 191 was greatly attenuated by concurrent exposure of cells to a mutagen interceptor, chlorophyllin (Pietrzak *et al.*, 2008). In another application, exposure of cells to supravital DNA probes such as Hoechst 33342 or DRAQ5 induced DDR that manifested as activation of ATM and Chk2 as well as phosphorylation of H2AX and p53 on Ser15, all or which is evidence of significant DNA damage (Zhao *et al.*, 2009b). Still another example of detection of genotoxic effects by this approach was the finding that the nitrogen oxide-releasing aspirine induces H2AX phosphorylation, ATM activation and leads to apoptosis of TK6 cells (Tanaka *et al.*, 2006e). This is an important observation since so modified aspirin, which as it appears from these data to have genotoxic properties, is being promoted as a novel anti-inflammatory agent.

### D. Oxidative DNA damage

DNA in live cells is continuously exposed to intracellular oxidants, the by-products of metabolic activity, as well as to exogenous oxidants or oxidant-inducers. The effect of such exposure is progressive oxidative DNA damage. It has been estimated that, during a single cell cycle of 24 h duration, the oxidants generate approximately 5,000 DNA single-strand lesions (SSLs) in the average cell in the human body (Vilenchik and Knudson, 2003). These

lesions are single-strand breaks, apurinic/apyrimidinic sites, oxidation products such as 8-oxoguanine and thymine glycol, and some alkylation products (Beckman and Ames, 1999). While about 99% of SSLs are repaired by essentially error-free mechanisms, one percent of them (~50) become converted to DSBs, predominantly during DNA replication. Recombinatorial repair (homologous recombination repair) and nonhomologous DNA-end joining (NHEJ) are the major pathways for repair of DSBs. The NHEJ pathway is error-prone, often resulting in deletion of a few base pairs (Pastwa and Blasik, 2003). This leads to an accumulation of DNA damage with each cell division. Such permanent damage is considered to be the primary cause of cell aging and senescence and promotes development of preneoplastic changes (Gorbunova and Seluanov, 2005). Strategies designed to slow down aging or prevent cancer often rely on protection of DNA from oxidative damage.

The presence of oxidants (Pham *et al.*, 2000) and certain DNA primary lesions resulting from oxidative damage detected immunocytochemically such as 8-oxoguanine (Cheng et al., 2003) can be assessed by cytometry. However, because of the scarcity of DSBs generated by endogenous oxidants, the possibilities for detecting them are limited. The comet methodology (Olive *et al.*, 2003) lacks the desired sensitivity. It also cannot provide information on the relationship between the presence of DSBs and the cell cycle phase or DNA ploidy of the cell being examined. We observed, however, that the background level of H2AX phosphorylation and activation of ATM seen in normal cells and cell lines during unperturbed growth, in the absence of any added exogenous genotoxic agents, is a reporter of the DNA damage induced by endogenous oxidants generated during aerobic respiration (Tanaka *et al.*, 2006a, 2006b, 2006c, 2007c, Zhao *et al.*, 2007). We defined this background level of H2AX phosphorylation and ATM activation as *constitutive DDR*. The level of constitutive DDR varies depending on the cell type (line) and on the phase of the cell cycle, being the highest for cells in S and $G_2$M phase. Given the same level of reactive oxidants detectable in a cell, the level of constitutive DDR differs depending on the status (wt, mutated or null) of TP53 (Tanaka *et al.*, 2006b).

Numerous experiments were designed to ensure that the constitutive DDR, revealed as the "background" H2AX phosphorylation and ATM activation in untreated cells, indeed is reporting DNA damage caused by endogenous oxidants. Initial experiments provided evidence that the level of H2AX phosphorylation and ATM activation can be markedly attenuated by exposure of cells to scavengers of reactive oxygen species (ROS) such as N-acetyl-L-cysteine (NAC) (Tanaka *et al.*, 2006a). The reduction in constitutive DDR was NAC-concentration dependent; the expression of γH2AX was reduced by 37–48% in cells exposed to NAC for only one hour (Fig. 9). In subsequent experiments we observed that a variety of factors that decreased the cell's metabolic rate such as growth in the presence of 2-deoxy-D-glucose or 3-bromopyruvate, hypoxic (3% $O_2$) conditions, or growth at low serum concentrations, all markedly reduced the constitutive level of expression of γH2AX and of activated ATM. Such a reduction was also seen after cell treatment with the antioxidant (vitamin C) (Tanaka *et al.*, 2006a, 2006c, Zhao *et al*., 2007). In contrast, the increased metabolic activity such as induced by mitogenic stimulation or treatment with dichloroacetate, an agent known to shift metabolism from anaerobic to oxidative glycolysis through its effect on pyruvate dehydrogenase kinase, enhanced the level of constitutive expression of γH2AX and activated ATM (Zhao *et al.*, 2007). Thus, all these data indicate that cytometric analysis of constitutive levels of H2AX phosphorylation and ATM activation offers the possibility of measuring the effectiveness of factors such as antioxidants, ROS scavengers or caloric restriction mimetics on protection of DNA from damage caused by endogenous or exogenous oxidants.

## VI. Interpretation of cytometric data. Role of image-assisted cytometry

The majority of applications in which cytometry is used to detect and measure DDR are directed towards evaluation of the extent of *actual DNA damage* caused by different genotoxins that would be predictive of potential mutagenic and cytotoxic consequences. Because DSBs represent the most deleterious DNA lesions, both in terms of their mutagenic potential as well as their role in providing the signal for activation cell death pathways, it is of importance to correlate the particular events of the DDR measured by cytometry with formation of DSBs. Initially, phosphorylation of H2AX on Ser139 was considered to be the specific marker of induction of DSBs. Indeed in instances of ionizing radiation and radiomimetic agents that directly generate DSBs, the intensity of expression of γH2AX, measured as the integrated fluorescence per nucleus (γH2AX IF) correlated well with the extent of DSBs. However, the expression of γH2AX after induction of DSBs is a kinetic event of relatively short duration. The expression of γH2AX on the other hand is not measured dynamically, in real time, but at an end-point at the time of cell harvest/fixation. Although in many instances γH2AX peaks at 1–2 h after induction of the DSB, the rate of its dephosphorylation varies markedly depending the cell cycle phase of the cell, the nature of the inducer of DSBs and the rate of DNA repair (Chowdhury *et al.*, 2005). As a result, there is uncertainty as to whether γH2AX IF is being measured at the "peak" of the response and thus whether the intensity of IF correlates well with the number of DSBs. Furthermore, there are instances such as following replication stress, when H2AX is phosphorylated (Kurose *et al.*, 2006a, 2006b) in the absence of DSBs (Ichijima *et al.*, 2010). Thus, the expression of γH2AX *per se* is not conclusive proof of the presence of DNA DSBs.

As mentioned earlier there is strong evidence that H2AX phosphorylation, triggered by formation of DSBs, is mediated by ATM (Burma *et al.*, 2001, Sedelnikova *et al.*, 2002). Therefore, when induction of γH2AX is accompanied by ATM activation, one is more assured that H2AX phosphorylation reports formation of DSBs. However there are instances such as during condensation of chromatin in mitosis (Ichijima *et al.*, 2005) or premature chromosome condensation (Huang *et al.*, 2006a) when both the expression of γH2AX and activation of ATM are seen and yet there is no straightforward evidence of formation of DSBs. Also, because of the redundancy of PIKKs in phosphorylation of different substrates, even when one of them is initially activated activation of other PIKKs may soon follow. We observed, for example that while after induction of DNA damage by UV activation of ATR is the first to be seen, activation of ATM shortly follows. One should be careful therefore with data interpretation because even when ATM activation and H2AX phosphorylation are observed to occur concurrently this may not necessarily be an assurance of the presence of DSBs.

The presence of distinct characteristic γH2AX or ATM-S1981$^P$ IF foci, each focus reported to represent a single DSB (Rogakou *et al.*,1998, 1999, Sedelnikova *et al.*, 2002), appears to be the most reliable marker of DSBs. The number of individual IF foci per nucleus, especially if double-labeled with ATM-S1981$^P$ and γH2AX (Tanaka *et al.*, 2006d) may provide a quantitative analysis of the number of DSBs induced in individual cells. This can be accomplished by image-assisted cytometric analysis utilizing, for example, a Laser Scanning Cytometer (LSC) (Darzynkiewicz *et al.*, 1999, Pozarowski *et al.*, 2005) or similar instruments (Fig. 10). Image analysis was shown to be able to detect very low levels of DNA damage, for example, as occurs *in vivo* in lymphocytes of patients subjected to computed tomography examinations (Lobrich *et al.*, 2005).

In practical terms, the count of individual foci per nucleus is limited to relatively small (<20) foci numbers. With greater numbers, foci proximity to each other and the possibility of their overlap create problems that may prevent accurate contouring. As is shown in Fig. 10, the

gating of cells with more than three foci per nucleus made it possible to identify them on DNA versus γH2AX distributions as having higher than the minimum level of γH2AX expression. However, many cells with the highest level of γH2AX were not selected by the gate (black dots, most in S-phase of the cell cycle). Identification of the cells by visual inspection using the LSC revealed that they had high numbers of foci, which led to overlapping of their contours that precluded foci quantification. Thus, quantification of foci by LSC works ideally fits when relatively few foci are present per nucleus such as during analysis of constitutive DNA damage response triggered by endogenous oxidants (Tanaka *et al.*, 2006a).

There are other issues that should also be considered when using image-assisted cytometry for foci quantification. Namely, the rates of phosphorylation and dephosphorylation of H2AX and/or ATM in individual foci in the same cell may vary depending on the rate of DNA repair at each particular DSB. Furthermore, when the induction of DSBs are asynchronous within the cell (for example as is the case of progressive DNA damage following treatment with low doses of genotoxins) the “age” and thus the IF intensity of individual foci may also vary. This variability in intensity of fluorescence of individual foci may complicate the setting optimal thresholds for contouring all foci.

## V. Role of microfluidic Lab-on-a-Chip platforms for DDR analysis

Advances in conventional flow and image-assisted cytometry provide the instrumentation of choice for studies requiring quantitative analysis of DDR. Surprisingly, however, commonly used high-content approaches are still based on the static principle, yielding information on the cell status at a particular time point. Capabilities of high-speed, multiparameter and real-time analysis of small numbers of patient derived cells are still very limited (Wlodkowic *et al.*, 2010). The improvements in such capabilities are of particular importance for the development of personalized therapeutic approaches (point-of-care diagnostics) and the increasing role of cost and time savings in drug screening pipelines. Not surprisingly, enabling strategies that can reduce expenditures while at the same time increase throughput and content of information are attracting growing interest (Wlodkowic *et al.*, 2010; Wlodkowic and Cooper, 2010).

The last decade, in particular, has brought some spectacular innovations in the field of miniaturized cytometric technologies that can open up new avenues for high-throughput DDR analysis. Namely, the up-and-coming microfluidic Lab-on-a-Chip (LOC) technology and the micro-total analysis systems (μTAS) are two of the most promising avenues for massively parallelized studies with single-cell resolution (Whitesides, 2006; El-Ali *et al.*, 2006; Sims and Allbritton, 2006). The transfer of traditional bioanalytical methods to a microfabricated format provides a means to reduce drug screening expenditures while vastly increasing throughput and content of information from a given sample (Manz and Dittrich, 2006). On the other hand, μTAS increase both the resolution of analysis while reducing the assay running costs (Hong *et al.*, 2009; Kang *et al.*, 2008). Most importantly, however, only small cell numbers and operational reagent volumes are required for microfabricated technologies as compared to the conventional counterparts such as e.g. flow cytometry (Sims and Allbritton, 2006; Wlodkowic *et al.*, 2009; Wlodkowic and Cooper, 2010). By providing an alternative to expensive instrumentation such as flow or laser scanning cytometers and sorters, user-friendly LOC technologies can prospectively enable routine DDR analysis on patient-derived specimens.

A number of emerging, microfluidic LOC technologies for cell-based assays has recently been reported such as microflow cytometry (μFCM), microfluorescently activated cell sorting (μFACS) and in-flow magnetically activated cell sorting (μMACS) that are all up-

and-coming examples of miniaturized on-chip flow cytometric technologies with substantial potential in DDR analysis and personalized diagnostics (Chan *et al.*, 2003; Wolff *et al.*, 2003; Fu *et al.*, 2002; Adams *et al.*, 2008). Microfluidic chip-based cytometry is slowly entering a commercial phase with increasing numbers of user-friendly devices capable of multiparameter fluorescent analysis of cells and particles (Wlodkowic *et al.*, 2009; Wlodkowic and Cooper, 2010). The most notable examples involve the CellLab Chip (Agilent Technologies, Santa Clara, CA, USA), Fishman-R (On-chip biotechnologies Co, Tokyo, Japan) and the Gigasort™ system (CytonomeST LLC, Boston, MA, USA) which all employ enclosed and disposable chip-based cartridges (Chan *et al.*, 2003; Wlodkowic *et al.*, 2009; Takeda and Jimma, 2009; Takao *et al.*, 2009). These approaches are particularly attractive for the clinical and diagnostic laboratories as they allow rapid analysis of only small amounts of patient derived cells.

Technological foundations initially developed for DNA microarrays have recently provided the starting point for development of chemical, protein microarrays, carbohydrate and tissue microarrays (Gomase *et al.*, 2008; Camp *et al.*, 2008; Ma and Horiuchi, 2006; Uttamchandani and Yao, 2008). They all offer miniaturization, low reagent consumption, automation as well as qualitative and quantitative approaches to analyze gene and protein expression on a population level (Sobek *et al.*, 2006). They do, however, suffer from a lack of capabilities to monitor single living cells in real-time and as such represent a binary system that averages the results from every given cell while capturing a snap-shot of the intermittent cellular reaction (Wlodkowic and Cooper, 2010; Wlodkowic *et al.*, 2010). These drawbacks have recently fueled the development of new technologies: the living cell microarrays and microfluidic cell arrays that advance the spatiotemporal control of biomolecules and cells (Yarmush and King, 2009; Wlodkowic and Cooper, 2010).

Cell microarrays in general allow creating positioned arrays composed of single living cells (DiCarlo *et al.*, 2006; Tokimitsu et al., 2007; Yamamura et al., 2005). Unlike flow cytometry, however, measurements are made at multiple time points, and in contrast to conventional time-lapse microscopy, image analysis is greatly simplified by arranging the cells in a spatially defined pattern and by their physical separation (DiCarlo *et al.*, 2006; Wlodkowic *et al.*, 2009; Wlodkowic and Cooper, 2010). As such they are ideal for drug screening routines and scalable for constructing high-throughput screening platforms (Wang *et al.*, 2007). They also have the ability to perform kinetic and multivariate analysis of signaling events on a single cell level (Wlodkowic *et al.*, 2009; Faley *et al.*, 2009). Thus, cell microarray technology seems to be particularly suitable to uncover intricacies in cell-to-cell variability and its relevance to cancer therapy including the DDR analysis at a single cell resolution (Wlodkowic and Cooper, 2010). In this context, our recent studies have validated the application of live-cell microarrays for the kinetic analysis of drug-induced programmed cell death in hematopoietic cancer cells and hematopoietic cancer stem cells (Wlodkowic *et al.*, 2009; Faley *et al.*, 2009). DDR analysis on living cell microarrays is a next logical example that can provide innovative diagnostic and screening applications.

We have recently postulated that the combination of microfluidic cell arrays with integrated on-chip gene delivery technology (geno*mics*), functional and dynamic live-cell analysis (cyt*omics*) and intracellular antibody staining of selected proteins (prote*omics*) can provide innovative, multivariate assays for high-content data mining and enhanced elucidation of cell signaling pathways (Wlodkowic *et al.*, 2010; Wlodkowic and Cooper, 2010). It is largely anticipated that advances in many innovative microfluidic technologies will provide innovative analytical tools for studies requiring quantitative analysis of the DDR.

## References


Abraham RT, Tibbetts RS. Guiding ATM to broken DNA. Science. 2005; 308:510–511. [PubMed: 15845843]

Adams JD, Kim U, Soh HT. Multitarget magnetic activated cell sorter. Proc. Natl. Acad. Sci. USA. 2008; 105:18165–18170. [PubMed: 19015523]

Ahn JY, Li X, Davis HL, Canman CE. Phosphorylation of threonine 68 promotes ologomerization and autophosphorylation of Chk2 protein kinase via the forkhead-associated domain. J. Biol. Chem. 2002; 277:19389–19395. [PubMed: 11901158]

Ahn J, Urist M, Prives C. The Chk2 protein kinase. DNA Repair. 2004; 3:1039–1047. [PubMed: 15279791]

Albino AP, Huang X, Jorgensen E, Gietl D, Traganos F, Darzynkiewicz Z. Induction of DNA double-strand breaks in A549 and normal human pulmonary epithelial cells by cigarette smoke is mediated by free radicals. Int. J. Oncol. 2006; 28:1491–1505. [PubMed: 16685450]

Albino AP, Huang X, Yang J, Gietl D, Jorgensen E, Traganos F, Darzynkiewicz Z. Induction of histone H2AX phosphorylation in A549 human pulmonary epithelial cells by tobacco smoke and in human bronchial epithelial cells by smoke condensate: A new assay to detect the presence of potential carcinogens in tobacco. Cell Cycle. 2004; 3:1062–1068. [PubMed: 15254392]

Albino AP, Jorgensen E, Rainey P, Gillman G, Clark TJ, Gietl D, Zhao H, Traganos F, Darzynkiewicz Z. γH2AX: A potential DNA damage response biomarker for assessing toxicological risk of tobacco products. Mutation Res. 2009; 678:43–52. [PubMed: 19591958]

Anderson L, Henderson C, Adachi Y. Phosphorylation and rapid relocalization of 53BP1 to nuclear foci upon DNA damage. Mol. Cell Biol. 2001; 21:1719–1729. [PubMed: 11238909]

Araujo FD, Stracker TH, Carson CT, Lee DV, Weitzman MD. Adenovirus type 5 E4orf3 protein targets the Mre11 complex to cytoplasmic aggresomes. J. Virol. 2005; 79:11382–11391. [PubMed: 16103189]

Bakkenist CJ, Kastan MB. DNA damage activates ATM through intermolecular autophosphorylation and dimer dissociation. Nature. 2003; 421:499–506. [PubMed: 12556884]

Bakkenist CJ, Kastan MB. Initiating cellular stress responses. Cell. 2004; 118:9–17. [PubMed: 15242640]

Banath JP, Olive PL. Expression of phosphorylated histone H2AX as a surrogate of cell killing by drugs that create DNA double-strand breaks. Cancer Res. 2003; 63:4347–4350. [PubMed: 12907603]

Banath JP, Macphail SH, Olive PL. Radiation sensitivity, H2AX phosphorylation, and kinetics of repair of DNA strand breaks in irradiated cervical cancer cells. Cancer Res. 2004; 64:7144–7148. [PubMed: 15466212]

Bassing CH, Suh H, Ferguson DO, Chua KF, Manis J, Eckersdorff M, Gleason M, Bronson R, Lee C, Alt FW. Histone H2AX: A dosage-dependent suppressor of oncogenic translocations in tumors. Cell. 2003; 114:359–370. [PubMed: 12914700]

Beckman KB, Ames BN. Oxidative decay of DNA. J. Biol. Chem. 1997; 272:13300–13305.

Bedner E, Li X, Kunicki J, Darzynkiewicz Z. Translocation of Bax to mitochondria during apoptosis measured by laser scanning cytometry. Cytometry. 2000; 41:83–88. [PubMed: 11002262]

Bonner WM, Redon CE, Dickey JS, Nakamura AJ, Sedelnikova OA, Solier S, Pommier Y. γH2AX and cancer. Nat. Rev. Cancer. 2008; 8:957–966. [PubMed: 19005492]

Boutros R, Dozier C, Ducommun B. The when and wheres of CDC25 phosphatases. Curr. Opin. Cell Biol. 2006; 18:185–191. [PubMed: 16488126]

Boutros R, Lobjois V, Ducommun B. CDC25 phosphatases in cancer cells: key players? Good targets? Nat. Rev. Cancer. 2007; 7:495–507. [PubMed: 17568790]

Burma S, Chen BP, Murphy M, Kurimasa A, Chen DJ. ATM phosphorylates histone H2AX in response to DNA double-strand breaks. J. Biol. Chem. 2001; 276:42462–42467. [PubMed: 11571274]

Camp RL, Neumeister V, Rimm DL. A decade of tissue microarrays: progress in the discovery and validation of cancer biomarkers. J. Clin. Oncol. 2008; 26:5630–5637. [PubMed: 18936473]

Celeste A, Difilippantonio S, Fernandez-Capetillo O, Pilch DR, Sedelnikova O, Eckhaus M, Ried T, Bonner WM, Nussenzweig A. H2AX haploinsufficiency modifies genomic stability and tumor susceptibility. Cell. 2003; 114:371–383. [PubMed: 12914701]

Chan DW, Chen, Chen BP, Prithivirajsingh S, Kurimasa A, Story MD, Qin J, Chen DJ. Autophosphorylation of the DNA-dependent protein kinase catalytic subunit is required for rejoining of DNA double-strand breaks. Genes Dev. 2002; 16:2333–2338. [PubMed: 12231622]

Chan SD, Luedke G, Valer M, Buhlmann C, Preckel T. Cytometric analysis of protein expression and apoptosis in human primary cells with a novel microfluidic chip-based system. Cytometry A. 2003; 55:119–125. [PubMed: 14505317]

Cheng TJ, Kao HP, Chan CC, Chang WP. Effects of ozone on DNA single-strand breaks and 8-oxoguanine formation in A549 cells. Environ. Res. 2003; 93:298–284.

Chowdhury D, Keogh MC, Ishii H, Peterson CL, Buratowski S, Lieberman J. gamma-H2AX dephosphorylation by protein phosphatase 2A facilitates DNA double-strand break repair. Mol. Cell. 2005; 20:801–809. [PubMed: 16310392]

Cuadrado, M.; Martinez-Pastor, B.; Fernandez-Capetillo, O. ATR activation in response to ionizing radiation: still ATM territory; Cell Division. 2006. p. 7http://www.celldiv.com/content/1/1/7

D'Arpa P, Beardmore C, Liu LF. Involvement of nucleic acid synthesis in cell killing mechanisms of topoisomerase poisons. Cancer Res. 1990; 50:6916–6924.

Darzynkiewicz Z. Acid-induced denaturation of DNA in situ as a probe of chromatin structure. Meth. Cell Biol. 1990; 33:337–352.

Darzynkiewicz Z, Bedner E, Gorczyca W, Melamed MR. Laser scanning cytometry. A new instrumentation with many applications. Exp. Cell Res. 1999; 249:1–12. [PubMed: 10328948]

Darzynkiewicz, Z.; Kapuscinski, J. Acridine Orange, a Versatile Probe of Nucleic Acids and Other Cell Constituents. In: Melamed, MR.; Mendelsohn, M.; Lindmo, T., editors. Flow Cytometry and Sorting. New York: Alan R. Liss, Inc.; 1990. p. 291-314.

Darzynkiewicz Z, Traganos F, Sharpless T, Melamed MR. Thermal denaturation of DNA *in situ* as studied by acridine orange staining and automated cytofluorometry. Exp Cell Res. 1975; 90:411–428. [PubMed: 46199]

Darzynkiewicz Z, Traganos F, Sharpless T, Melamed MR. Different sensitivity of DNA *in situ* in interphase and metaphase chromatin to heat denaturation. J. Cell Biol. 1977; 73:128–138. [PubMed: 16017]

Darzynkiewicz Z, Traganos F, Wlodkowic D. Impaired DNA damage response – an Achilles'heel sensitizing cancer to chemotherapy and radiotherapy. Eur. J. Pharmacol. 2009; 625:143–150. [PubMed: 19836377]

Di Carlo D, Wu LY, Lee LP. Dynamic single cell culture array. Lab. Chip. 2006; 6:1445–1449. [PubMed: 17066168]

Dobrucki J, Darzynkiewicz Z. Chromatin condensation and sensitivity of DNA *in situ* to denaturation during cell cycle and apoptosis. A confocal microscopy study. Micron. 2001; 32:645–652. [PubMed: 11334733]

Downs JA, Cote J. Dynamics of chromatin during the repair of DNA double-strand breaks. Cell Cycle. 2005; 4:1373–1376. [PubMed: 16205111]

El-Ali J, Sorger PK, Jensen KF. Cells on chips. Nature. 2006; 442:403–411. [PubMed: 16871208]

Evenson DP, Darzynkiewicz Z, Melamed MR. Relation of mammalian sperm chromatin heterogeneity to fertility. Science. 1980; 210:1131–1133. [PubMed: 7444440]

Faley SL, Copland M, Wlodkowic D, Kolch W, Seale KT, Wikswo JP, Cooper JM. Microfluidic single cell arrays to interrogate signalling dynamics of individual, patient-derived hematopoietic stem cells. Lab. Chip. 2009; 9:2659–2664. [PubMed: 19704981]

Fu AY, Chou HP, Spence C, Arnold FH, Quake SR. An integrated microfabricated cell sorter. Anal. Chem. 2002; 74:2451–2457. [PubMed: 12069222]

Furuta T, Takemura H, Liao Z-Y, Aune GJ, Redon C, Sedelnikova OA, Pilch DR, Rogakou EP, Celeste A, Chen HT, Nussenzweig A, Aladjem MI, Bonner WM, Pommier Y. Phosphorylation of histone H2AX and activation of Mre11, Rad50, and Nbs1 in response to replication-dependent DNA double-strand breaks induced by mammalian topoisomerase I cleavage complexes. J. Biol. Chem. 2003; 278:20303–20312. [PubMed: 12660252]

Gerlitz G, Bustin M. Nucleosome binding proteins potentiate ATM activation and DNA damage response by modifying chromatin. Cell Cycle. 2009; 8:1641–1644. [PubMed: 19411861]

Gomase VS, Tagore S, Kale KV. Microarray: an approach for current drug targets. Curr. Drug Metab. 2008; 9:221–231. [PubMed: 18336225]

Gorczyca W, Traganos F, Jesionowska H, Darzynkiewicz Z. Presence of DNA strand breaks and increased sensitivity of DNA *in situ* to denaturation in abnormal human sperm cells. Analogy to apoptosis of somatic cells. Exp. Cell Res. 1993; 207:202–205. [PubMed: 8391465]

Gorbunova V, Seluanov A. Making ends meet in old age: DSB repair and aging. Mech. Ageing Dev. 2005; 126:621–628. [PubMed: 15888314]

Halicka HD, Huang X, Traganos F, King MA, Dai W, Darzynkiewicz Z. Histone H2AX phosphorylation after cell irradiation with UV-B: Relationship to cell cycle phase and induction of apoptosis. Cell Cycle. 2005; 4:339–345. [PubMed: 15655354]

Halicka HD, Ozkaynak MF, Levendoglu-Tugal O, Sandoval C, Seiter K, Kajstura M, Traganos F, Jaybose S, Darzynkiewicz Z. DNA damage response as a biomarker in treatment of leukemias. Cell Cycle. 2009a; 8:1720–1724. [PubMed: 19411853]

Halicka HD, Zhao H, Podhorecka M, Traganos F, Darzynkiewicz Z. Cytometric detection of chromatin relaxation, an early reporter of DNA damage response. Cell Cycle. 2009b; 8:2233–2237. [PubMed: 19502789]

Hanasoge S, Ljungman M. H2AX phosphorylation after UV irradiation is triggered by DNA repair intermediates and is mediated by the ATR kinase. Carcinogenesis. 2007; 28:2298–2304. [PubMed: 17615256]

Helt CE, Cliby WA, Keng PC, Bambara RA, O'Reilly MA. Ataxia telangiectasia mutated (ATM) and ATM and Rad3-related protein exhibit selective target specificities in response to different forms of DNA damage. J. Biol. Chem. 2005; 280:1186–1192. [PubMed: 15533933]

Hill R, Lee PWK. The DNA-dependent protein kinase (DNA-PK). More than just a case of making ends meet? Cell Cycle. 2010; 9:3460–3469. [PubMed: 20855954]

Hong J, Edel JB, deMello AJ. Micro- and nanofluidic systems for high-throughput biological screening. Drug Discov. Today. 2009; 14:134–146. [PubMed: 18983933]

Hsiang YH, Lihou MG, Liu LF. Arrest of replication forks by drug stabilized topoisomeraseI-DNA cleavable complexes as a mechanism of cell killing by camptothecin. Cancer Res. 1989; 49:5077–5082. [PubMed: 2548710]

Huang X, Kurose A, Tanaka T, Traganos F, Dai W, Darzynkiewicz Z. Sequential phosphorylation of Ser-10 on histone H3 and Ser-139 on histone H2AX and ATM activation during premature chromosome condensation: Relationship to cell-cycle and apoptosis. Cytometry A. 2006a; 69A: 222–229.

Huang X, Kurose A, Tanaka T, Traganos F, Dai W, Darzynkiewicz Z. Activation of ATM and histone H2AX phosphorylation induced by mitoxantrone but not by topotecan is prevented by the antioxidant N-acetyl-L-cysteine. Cancer Biol. Ther. 2006b; 5:959–964. [PubMed: 16760673]

Huang X, Okafuji M, Traganos F, Luther E, Holden E, Darzynkiewicz Z. Assessment of histone H2AX phosphorylation induced by DNA topoisomerase I and II inhibitors topotecan and mitoxantrone and by DNA crosslinking agent cisplatin. Cytometry A. 2004; 58A:99–110. [PubMed: 15057963]

Huang X, Traganos F, Darzynkiewicz Z. DNA damage induced by DNA topoisomerase I- and topoisomerase II- inhibitors detected by histone H2AX phosphorylation in relation to the cell cycle phase and apoptosis. Cell Cycle. 2003; 2:614–619. [PubMed: 14504478]

Ichijima Y, Sakasai R, Okita N, Asahina K, Mizutani S, Teraoka H. Phosphorylation of histone H2AX at M phase in human cells without DNA damage response. Biochem. Biophys. Res. Commun. 2005; 336:807–812. [PubMed: 16153602]

Ichijima Y, Yoshioka K, Yoshioka Y, Shinohe K, Fujimori H, Unno M, Goto H, Inagaki M, Mizutani S, Teraoka H. DNA lesions induced by replication stress trigger mitotic aberration and tetraploidy development. PLoS One. 2010 Jan 21.5(1):e8821. [PubMed: 20098673]

Ikura T, Tashiro S, Kakino A, Shima H, Jacob N, Amunugama R, Yoder K, Izumi S, Kuraoka I, Tanaka K, Kimura H, Ikura M, Nishikubo S, Ito T, Muto A, Miyagawa K, Takeda S, Fishel R,

Igarashi K, Kamiya K. DNA damage dependent acetylation and ubiquitination of H2AX enhances chromatin dynamics. Mol. Cell Biol. 2007; 27:7028–7040. [PubMed: 17709392]

Jackson SP. DNA damage signaling and apoptosis. Biochem. Soc. Transactions. 2001; 29:655–661.

Jorgensen ED, Zhao H, Traganos F, Albino AP, Darzynkiewicz Z. DNA damage response induced by exposure of A549 human lung adenocarcinoma cells to smoke from tobacco- and nicotine-free cigarettes. Cell Cycle. 2010; 9:2170–2176. [PubMed: 20404482]

Juan G, Traganos F, James WM, Ray JM, Roberge M, Sauve DM, Darzynkiewicz Z. Histone H3 phosphorylation and expression of cyclins A and B1 measured in individual cells during their progression through G2 and mitosis. Cytometry. 1998; 32:71–77. [PubMed: 9627219]

Kamentsky LA, Kamentsky LD, Fletcher JA, Kurose A, Sasaki K. Methods for automatic multiparameter analysis of fluorescence in situ hybridized specimens with laser scanning cytometer. Cytometry. 1997; 27:117–125. [PubMed: 9012378]

Kang L, Chung B, Langer R, Khademhosseini A. Microfluidics for drug discovery and development: from target selection to product lifecycle management. Drug Discov. Today. 2008; 13:1–13. [PubMed: 18190858]

Kapuscinski J, Darzynkiewicz Z. Condensation of nucleic acids by intercalating aromatic cations. Proc. Natl. Acad. Sci. USA. 1984a; 81:7368–7372. [PubMed: 6209715]

Kapuscinski J, Darzynkiewicz Z. Denaturation of nucleic acids induced by intercalating agents. Biochemical and biophysical properties of acridine orange-DNA complexes. J. Biomol. Struct. Dyn. 1984b; 1:1485–1499. [PubMed: 6400830]

Kapuscinski J, Darzynkiewicz Z. Relationship between the pharmacological activity of antitumor drugs Ametantrone and Mitoxantrone (Novantrone) and their ability to condense nucleic acids. Proc. Natl. Acad. Sci. USA. 1986; 83:6302–6306. [PubMed: 3462696]

Kastan MB. DNA damage responses: Mechanisms and roles in human disease. 2007 G.H.A. Cloves Memorial Award Lecture. Mol. Cancer Res. 2008; 6:517–524. [PubMed: 18403632]

Kim YC, Gerlitz G, Furusawa T, Catez F, Nussenzweig A, Oh KS, Kraemer KH, Shiloh Y, Bustin M. Activation of ATM depends on chromatin interactions occurring before induction of DNA damage. Nat. Cell Biol. 2009; 11:92–96. [PubMed: 19079244]

Kingma PS, Burden DA, Osheroff N. Binding of etoposide to topoisomerase II in the absence of DNA: decreased affinity as a mechanism of drug resistance. Biochemistry. 1999; 38:3457–3461. [PubMed: 10090731]

Kitagawa R, Kastan MB. The ATM-dependent DNA damage signaling pathway. Cold Spring Harb. Symp. Quant. Biol. 2005; 70:99–109. [PubMed: 16869743]

Kitagawa R, Bakkenist CJ, McKinnon PJ, Kastan MB. Phosphorylation of SMC1 is a critical downstream event in the ATM-ANBS1-BRCA1 pathway. Genes Dev. 2004; 18:1423–1438. [PubMed: 15175241]

Kruhlak MJ, Celeste A, Nussenzweig A. Spatio-temporal dynamics of chromatin containing DNA breaks. Cell Cycle. 2006; 5:1910–1912. [PubMed: 16929171]

Kurose A, Tanaka T, Huang X, Halicka HD, Traganos F, Dai W, Darzynkiewicz Z. Assessment of ATM phosphorylation on *Ser*-1981 induced by DNA topoisomerase I and II inhibitors in relation to *Ser*-139-histone H2AX phosphorylation, cell cycle phase and apoptosis. Cytometry A. 2005; 68A:1–9. [PubMed: 16184611]

Kurose A, Tanaka T, Huang X, Traganos F, Dai W, Darzynkiewicz Z. Effects of hydroxyurea and aphidicolin on phosphorylation of ATM on *Ser* 1981 and histone H2AX on *Ser* 139 in relation to cell cycle phase and induction of apoptosis. Cytometry A. 2006a; 69A:212–221.

Kurose A, Tanaka T, Huang X, Traganos F, Darzynkiewicz Z. Synchronization in the cell cycle by inhibitors of DNA replication induces histone H2AX phosphorylation, an indication of DNA damage. Cell Prolif. 2006b; 39:231–240. [PubMed: 16672000]

Lee JH, Paull TT. ATM activation by DNA double-strand breaks through the Mre11-Rad50-Nbs1 complex. Science. 2005; 308:551–554. [PubMed: 15790808]

Lee JS, Collins KM, Brown AL, Lee CH, Chung JH. hCds1-mediated phosphorylation of BRCA1 regulates the DNA damage response. Nature. 2000; 404:201–204. [PubMed: 10724175]

Li J, Stern DF. DNA damage regulates Chk2 association with chromatin. J. Biol. Chem. 2005; 280:37948–37956. [PubMed: 16150728]

Li L, Zou L. Sensing signaling and responding to DNA damage: organization of checkpoint pathways in mammalian cells. J. Cell Biochem. 2005; 94:298–306. [PubMed: 15578575]

Lim J, Catez F, Birger Y, West K, Prymakowska-Bosak M, Postnikov MV, Bustin M. Chromosomal protein HMGN1 modulates histone H3 phosphorylation. Mol. Cell. 2004; 15:573–584. [PubMed: 15327773]

Lin J, Reichner C, Wu X, Levine AJ. Analysis of wild-type and mutant p21WAF-1 gene activities. Mol. Cell Biol. 1996; 16:1786–1793. [PubMed: 8657154]

Lobrich M, Rief N, Kuhne M, Heckman M, Fleckensstein J, Rube C, Uder M. *In vivo* formation and repair of DNA double-strand breaks after computed tomography examinations. Proc. Natl. Acad. Sci. USA. 2005; 102:8994–8989.

Lovejoy CA, Cortez D. Common mechanisms of PIKK regulation. DNA Repair. 2009; 8:1004–1008. [PubMed: 19464237]

Ma H, Horiuchi KY. Chemical microarray: a new tool for drug screening and discovery. Drug Discov. Today. 2006; 11:661–668. [PubMed: 16793536]

MacPhail SH, Banath JP, Yu TY, Chu EH, Lambur H, Olive PL. Expression of phosphorylated histone H2AX in cultured cell lines following exposure to X-rays. Int. J. Radiat. Biol. 2003a; 79:351–358. [PubMed: 12943243]

MacPhail SH, Banath JP, Yu Y, Chu E, Olive PL. Cell cycle-dependent expression of phosphorylated histone H2AX: reduced expression in unirradiated but not X-irradiated G1-phase cells. Radiat. Res. 2003b; 159:759–767. [PubMed: 12751958]

Manz A, Dittrich PS. Lab-on-a-chip: microfluidics in drug discovery. Nature Drug Discovery. 2006; 5:210–218.

Marko JF. Linking topology to large DNA molecules. Physica A. 2010; 389:2997–3001. [PubMed: 20606760]

Marti TM, Hefner E, Feeney L, Natale V, Cleaver JE. H2AX phosphorylation within the G1 phase after UV irradiation depends on *nucleotide excision repair and not DNA double-strand breaks*. Proc. Natl. Acad. Sci. USA. 2006; 103:9891–9896. [PubMed: 16788066]

Matsuoka S, Rotman G, Ogawa A, Shiloh K, Tamai SJ, Elledge SJ. Ataxia telangiectasia-mutated phosphorylates Chk2 in vivo and in vitro. Proc. Natl. Acad. Sci. USA. 2000; 97:10289–10394.

Misteli T, Soutoglou E. The emerging role of nuclear architecture in DNA repair and genome maintenance. Mol. Cell Biol. 2009; 10:243–254.

Modesti M, Kanaar R. DNA repair: spot(light)s on chromatin. Curr. Biol. 2001; 11:R229–R232. [PubMed: 11301269]

Murga M, Jaco I, Soria R, Martinez-Pastor B, Cuadrado M, Yang S-M, Blasco MA, Skoultchi AI, Fernandez-Capetillo O. Global chromatin compaction limits the strength of the DNA damage response. J. Cell Biol. 2007; 178:1101–1108. [PubMed: 17893239]

Nakamura AJ, Rao VA, Pommier Y, Bonner WM. The complexity of phosphorylated H2AX foci formation and DNA repair assembly at DNA double-strand breaks. Cell Cycle. 2010; 9:389–398. [PubMed: 20046100]

Olive PL. Detection of DNA damage in individual cells by analysis of histone H2AX phosphorylation. Meth. Cell Biol. 2005; 75:355–375.

Olive PL, Banath JP. Phosphorylation of histone H2AX as a measure of radiosensitivity. Int. J. Radiat. Oncol. Biol. Phys. 2004; 58:331–335. [PubMed: 14751500]

Olive PG, Banath JP. Kinetics of HAX phosphorylation after exposure to cisplatin. Cytometry B Clin. Cytom. 2009; 76:79–90. [PubMed: 18727058]

Olive PL, Banath JP, Sinnott LT. Phosphorylated histone H2AX in spheroids, tumors, and tissues of mice exposed to etoposide and 3-amino-1,2,4-benzotriazine-1,3-dioxide. Cancer Res. 2004; 64:5363–5369. [PubMed: 15289343]

Olive PL, Durand RE, Banath JP, Johnston PJ. Analysis of DNA damage in individual cells. Methods Cell Biol. 2001; 64:235–249. [PubMed: 11070842]

Pandita TK, Richardson C. Chromatin remodeling finds its place in the DNA double-strand breaks. Nucleic Acids Res. 2009; 37:1363–1377. [PubMed: 19139074]

Park EJ, Chan DW, Park JH, Oettinger MA, Kwon J. DNA-PK is activated by nucleosomes and phosphorylated H2AX within the nucleosomes in an acetylation-dependent manner. Nucleic Acids Res. 2003; 31:6819–6827. [PubMed: 14627815]

Pastwa E, Blasiak J. Nonhomologous DNA end joining. Acta Biochim. Pol. 2003; 50:891–908. [PubMed: 14739985]

Paull TT, Lee JH. The Mre11/Rad50/Nbs1 complex and its role as a DNA-double strand break sensor for ATM. Cell Cycle. 2005; 4:737–740. [PubMed: 15908798]

Pham NA, Robinson BH, Hedley DW. Simultaneous detection of mitochondrial respiratory chain activity and reactive oxygen in digitonin-permeabilized cells using flow cytometry. Cytometry. 2000; 41:245–251. [PubMed: 11084609]

Pietrzak M, Halicka HD, Wieczorek Z, Wieczorek J, Darzynkiewicz Z. Attenuation of acridine mutagen ICR 191-DNA interactions and DNA damage by the mutagen interceptor chlorophyllin. Biophys. J. 2008; 135:69–75.

Pozarowski P, Holden E, Darzynkiewicz Z. Laser scanning cytometry. Principles and applications. Meth. Molec. Biol. 2005; 319:165–192.

Rogakou EP, Boon C, Redon C, Bonner WM. Megabase chromatin domains involved in DNA double-strand breaks *in vivo*. J. Cell Biol. 1999; 146:905–916. [PubMed: 10477747]

Rogakou EP, Pilch DR, Orr AH, Ivanova VS, Bonner WM. DNA double-stranded breaks induce histone H2AX phosphorylation on serine 139. J. Biol. Chem. 1998; 273:5858–5868. [PubMed: 9488723]

Rouleau M, Aubin RA, Poirier GG. Poly(ADP-ribosyl)ated chromatin domains: access granted. J. Cell Sci. 2004; 117:815–825. [PubMed: 14963022]

Rudolph J. Cdc25 phosphatases: Structure, specificity and mechanism. Biochemistry. 2007; 46:3595–3604. [PubMed: 17328562]

Rubi CP, Milner J. p53 is a chromatin accessibility factor for nucleotide excision repair of DNA damage. The EMBO J. 2003; 22:975–986.

Salic A, Mitchison TJ. A chemical method for fast and sensitive detection of DNA synthesis in vivo. Proc. Natl. Acad. Sci. USA. 2008; 105:2415–2420. [PubMed: 18272492]

Samper E, Goytisolo EA, Slijepcevic P, van Buul PP, Blasco MA. Mammalinan Ku86 protein prevents telomeric fusions independently of the length of TTAGGG repeats and the G-strand overhang. EMBO Rep. 2000; 1:244–252. [PubMed: 11256607]

Sedelnikova OA, Rogakou EP, Panuytin IG, Bonner W. Quantitive detection of 125IUdr-induced DNA double-strand breaks with γ-H2AX antibody. Ratiation Res. 2002; 158:486–492.

Shiloh Y. ATM and related protein kinases: safeguarding genome integrity. Nat. Rev. Cancer. 2003; 22:5834–5868.

Sims CE, Allbritton NL. Analysis of single mammalian cells on-chip. Lab. Chip. 2007; 7:423–440. [PubMed: 17389958]

Sinha RP, Häder D-P. UV-induced DNA damage and repair: A review. Photochem. Photobiol. Sci. 2002; 1:225–236. [PubMed: 12661961]

Sinha M, Peterson CL. Chromatin dynamics during repair of chromosomal DNA double-strand breaks. Epigenomics. 2009; 1:371–385. [PubMed: 20495614]

Smart DJ, Halicka HD, Schmuck G, Traganos F, Darzynkiewicz Z, Williams GM. Assessment of DNA double-strand breaks and γH2AX induced by the topoisomerase II poisons etoposide and mitoxantrone. Mutat. Res. 2008; 641:43–47. [PubMed: 18423498]

Smith GR. How homologous recombination is initiated: unexpected evidence for single-strand nicks from v(d) site-specific recombination. Cell. 2004; 117:146–148. [PubMed: 15084252]

Smith GC, Jackson SP. The DNA-dependent protein kinase. Genes Dev. 1999; 13:916–934. [PubMed: 10215620]

Sobek J, Bartscherer K, Jacob A, Hoheisel JD, Angenendt P. Microarray technology as a universal tool for high-throughput analysis of biological systems. Comb. Chem. High Throughput Screen. 2006; 9:365–380. [PubMed: 16787150]

Stevens C, Smith L, La Thangue NB. Chk2 activates E2F-1 in response to DNA damage. Nat. Cell Biol. 2003; 5:4465–4479.

Stokes MP, Rush J, MavNeill J, Ren JM, Sprott K, Nardone J, Yang V, Beausoleil SA, Gygi SP, Livingstone M, Zhang H, Polakiewicz RD, Comb MJ. Profilling of UV-induced ATM/ATR signalling pathways. Proc. Natl. Acad. Sci. USA. 2007; 104:19855–19860. [PubMed: 18077418]

Stucki M, Jackson SP. MDC1/NFBD1: a key regulator of the DNA damage response in higher eukaryotes. DNA Repair (Amst.). 2005; 3:953–957. [PubMed: 15279781]

Sun Y, Jiang X, Chen S, Fernandes N, Price BD. A role for the Tip60 histone acetyltransferase in the acetylation and activation of ATM. Proc. Natl. Acad. Sci. USA. 2005; 102:13182–13187. [PubMed: 16141325]

Takao M, Jimma F, Takeda K. Expanded applications of new-designed microfluidic flow cytometer (FISHMAN-R). Cytometry B. 2009; 76B:405–406.

Takeda K, Jimma F. Maintenance free biosafety flowcytometer using disposable microfluidic chip (FISHMAN-R). Cytometry B. 2009; 76B:405–406.

Tan Y, Raychaudhuri P, Costa RH. Chk2 mediates stabilization of the FoxM1 transcription factor to stimulate expression of DNA repair genes. Mol. Cell Biol. 2007; 27:1007–1016. [PubMed: 17101782]

Tanaka T, Halicka HD, Huang X, Traganos F, Darzynkiewicz Z. Constitutive histone H2AX phosphorylation and ATM activation, the reporters of DNA damage by endogenous oxidants. Cell Cycle. 2006a; 5:1940–1945. [PubMed: 16940754]

Tanaka T, Halicka HD, Traganos F, Seiter K, Darzynkiewicz Z. Induction of ATM activation, histone H2AX phosphorylation and apoptosis by etoposide: Relation to the cell cycle phase. Cell Cycle. 2007c; 6:371–376. [PubMed: 17297310]

Tanaka T, Huang X, Halicka HD, Zhao H, Traganos F, Albino AP, Dai W, Darzynkiewicz Z. Cytometry of ATM activation and histone H2AX phosphorylation to estimate extent of DNA damage induced by exogenous agents. Cytometry A. 2007a; 71A:648–661.

Tanaka T, Huang X, Jorgensen E, Gietl E, Traganos F, Darzynkiewicz Z, Albino AP. ATM activation accompanies histone H2AX phosphorylation in A549 cells upon exposure to tobacco smoke. BMC Cell Biol. 2007b Epub June 26, 8:26.

Tanaka T, Kajstura M, Halicka HD, Traganos F, Darzynkiewicz Z. Constitutive histone H2AX phosphorylation and ATM activation are strongly amplified during mitogenic stimulation of lymphocytes. Cell Prolif. 2007c; 40:1–13. [PubMed: 17227291]

Tanaka T, Kurose A, Halicka HD, Huang X, Traganos F, Darzynkiewicz Z. Nitrogen oxide-releasing aspirin induces histone H2AX phosphorylation, ATM activation, and apoptosis preferentially in S-phase cells; involvement of reactive oxygen species. Cell Cycle. 2006e; 5:1669–1674. [PubMed: 16861926]

Tanaka T, Kurose A, Huang X, Dai W, Darzynkiewicz Z. ATM kinase activation and histone H2AX phosphorylation as indicators of DNA damage by DNA topoisomerase I inhibitor topotecan and during apoptosis. Cell Prolif. 2006d; 39:49–60. [PubMed: 16426422]

Tanaka T, Kurose A, Halicka HD, Traganos F, Darzynkiewicz Z. 2-Deoxy-(2006c) D-glucose reduces the level of constitutive activation of ATM and phosphorylation of histone H2AX. Cell Cycle. 5:878–882. [PubMed: 16628006]

Tanaka T, Kurose A, Huang X, Traganos F, Dai W, Darzynkiewicz Z. Extent of constitutive histone H2AX phosphorylation on *Ser*-139 varies in cells with different TP53 status. Cell Prolif. 2006b; 39:313–323. [PubMed: 16872365]

Thatcher TH, Gorovsky MA. Phylogenetic analysis of the core histones H2A, H2B, H3 and H4. Nucleic Acids Res. 1994; 22:174–183. [PubMed: 8121801]

Tokimitsu Y, Kishi H, Kondo S, Honda R, Tajiri K, Motoki K, Ozawa T, Kadowaki S, Obata T, Fujiki S, Tateno C, Takaishi H, Chayama K, Yoshizato K, Tamiya E, Sugiyama T, Muraguchi A. Single lymphocyte analysis with a microwell array chip. Cytometry A. 2007; 71:1003–1010. [PubMed: 17972305]

Uttamchandani M, Yao SQ. Peptide microarrays: next generation biochips for detection, diagnostics and high-throughput screening. Curr. Pharm. Des. 2008; 14:2428–2438. [PubMed: 18781992]

Vilenchik MM, Knudson AG. Endogenous DNA double-strand breaks: Production, fidelity of repair, and induction of cancer. Proc. Natl. Acad. Sci. USA. 2003; 100:12871–12876. [PubMed: 14566050]

Wakeman TP, Kim WJ, Callens S, Chu A, Brown KD, Xu B. The ATM-SMC1 pathway is essential for activation of chromium [VI]-induced S-phase checkpoint. Mutat. Res. 2004; 554:241–251. [PubMed: 15450422]

Wang J, Chin MY, Li G. The novel tumor suppressor p33ING2 enhances nucleotide excision repair via inducement of histone H4 acetylation and chromatin relaxation. Cancer Res. 2006; 66:1906–1911. [PubMed: 16488987]

Wang Z, Kim MC, Marquez M, Thorsen T. High-density microfluidic arrays for cell cytotoxicity analysis. Lab. Chip. 2007; 7:740–745. [PubMed: 17538716]

Ward IM, Minn K, Chen J. UV-induced ataxia-telangiectasia-mutated and Rad3-related (ATR) activation requires replication stress. J. Biol. Chem. 2004; 279:9677–9680. [PubMed: 14742437]

Whitesides GM. The origins and the future of microfluidics. Nature. 2006; 442:368–372. [PubMed: 16871203]

Wlodkowic D, Cooper JM. Microfabricated analytical systems for integrated cancer cytomics. Anal. Bioanal. Chem. 2010; 398:193–209. [PubMed: 20419489]

Wlodkowic D, Cooper JM. Microfluidic cell arrays in tumor analysis: new prospects for integrated cytomics. Expert Rev. Mol. Diagn. 2010; 10:521–530. [PubMed: 20465506]

Wlodkowic D, Faley S, Zagnoni M, Wikswo JP, Cooper JM. Microfluidic single-cell array cytometry for the analysis of tumor apoptosis. Anal. Chem. 2009; 81:5517–5523. [PubMed: 19514700]

Wlodkowic D, Skommer J, Darzynkiewicz Z. Cytometry in cell necrobiology revisited. Recent advances and new vistas. Cytometry A. 2010; 77A:591–606. [PubMed: 20235235]

Wlodkowic D, Skommer J, Faley S, Darzynkiewicz Z, Cooper JM. Dynamic analysis of apoptosis using cyanine SYTO probes: from classical to microfluidic cytometry. Exp. Cell Res. 2009; 315:1706–1714. [PubMed: 19298813]

Wolff A, Perch-Nielsen IR, Larsen UD, Friis P, Goranovic G, Poulsen CR, Kutter JP, Telleman P. Integrating advanced functionality in a microfabricated high-throughput fluorescent-activated cell sorter. Lab. Chip. 2003; 3:22–27. [PubMed: 15100801]

Yajima H, Lee KJ, Zhang S, Kobayashi J, Chen BP. DNA double-strand break formation upon UV-induced replication stress activates ATM and DNA-PKcs kinases. J. Mol. Biol. 2009; 385:800–810. [PubMed: 19071136]

Yamamura S, Kishi H, Tokimitsu Y, Kondo S, Honda R, Rao SR, Omori M, Tamiya E, Muraguchi A. Single-cell microarray for analyzing cellular response. Anal. Chem. 2005; 77:8050–8056. [PubMed: 16351155]

Yang S, Kuo C, Bisi JE, Kim MK. PML-dependent apoptosis after DNA damage is regulated by the checkpoint kinase hCdsa/Chk2. Nat. Cell Biol. 2002; 4:865–870. [PubMed: 12402044]

Yarmush ML, King KR. Living-cell microarrays. Annu. Rev. Biomed. Eng. 2009; 11:235–257. [PubMed: 19413510]

Yuan SS, Lee SE, Chen G, Song M, Tomlinson GE, Lee FY. BRCA2 is required for ionizing radiation-induced assembly of Rad51 complex in vivo. Cancer Res. 1999; 59:3547–3551. [PubMed: 10446958]

Zhao H, Albino AP, Jorgensen E, Traganos F, Darzynkiewicz Z. DNA damage response induced by tobacco smoke in normal human bronchial epithelial and A549 pulmonary adenocarcinoma cells assessed by laser scanning cytometry. Cytometry A. 2009a; 75A:840–847.

Zhao H, Tanaka T, Halicka HD, Traganos F, Zarebski M, Dobrucki J, Darzynkiewicz Z. Cytometric assessment of DNA damage by exogenous and endogenous oxidants reports the aging-related processes. Cytometry A. 2007; 71A:905–914. [PubMed: 17879239]

Zhao H, Traganos F, Albino AP, Darzynkiewicz Z. Oxidative stress induces cell cycle-dependent Mre11 recruitment, ATM and Chk2 activation and histone H2AX phosphorylation. Cell Cycle. 2008a; 7:1490–1495. [PubMed: 18418078]

Zhao H, Traganos F, Darzynkiewicz Z. Phosphorylation of p53 on *Ser*15 during cell cycle caused by Topo I and Topo II inhibitors in relation to ATM and Chk2 activation. Cell Cycle. 2008b; 7:3048–3055. [PubMed: 18802408]

Zhao H, Traganos F, Darzynkiewicz Z. Kinetics of histone H2AX phosphorylation and Chk2 activation in A549 cells treated with topotecan and mitoxantrone in relation to the cell cycle phase. Cytometry A. 2008c; 73A:480–489.

Zhao H, Traganos F, Darzynkiewicz Z. Kinetics of the UV-induced DNA damage response in relation to cell cycle phase. Correlation with DNA replication. Cytometry A. 2010; 77A:285–293. [PubMed: 20014310]

Zhao H, Traganos F, Dobrucki J, Wlodkowic D, Darzynkiewicz Z. Induction of DNA damage response by the supravital probes of nucleic acids. Cytometry A. 2009b; 75A:510–519.

Zhang Q, Wang Y. High mobility group proteins and their post-transcriptional modifications. Biochim. Biophys. Acta. 2008; 1794:1159–1166. [PubMed: 18513496]

Zhou BB, Elledge SJ. The DNA response: putting checkpoints in perspective. Nature. 2000; 408:433–439. [PubMed: 11100718]

Ziv Y, Bielopolski D, Galanty Y, Lukas C, Taya Y, Schultz DC, Lukas J, Bekker-Jensen S, Bartek J, Shiloh Y. Chromatin relaxation in response to DNA double-strand breaks is modulated by a novel ATM-and KAP-1 dependent pathway. Nat. Cell Biol. 2006; 8:870–876. [PubMed: 16862143]

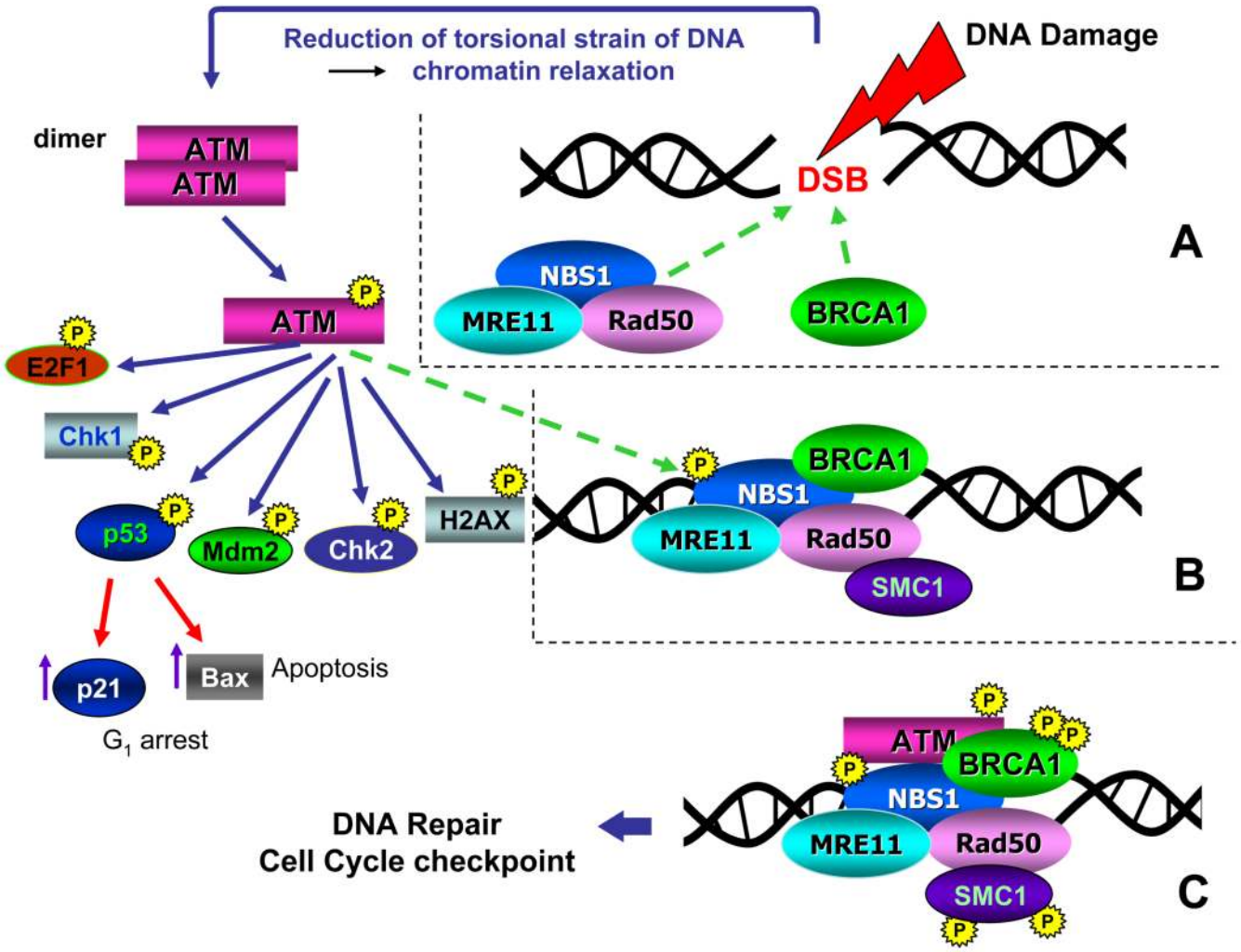


**Fig. 1. The ATM signaling pathway triggered by induction of DSBs [(Kitagawa *et al.* (2004), updated (Darzynkiewicz *et al.*, 2009)]**

Induction of DSB leads to lessening of torsional strain and unwinding of DNA superhelical structure which triggers local decondensation of chromatin and recruits the MRE11, RAD50 and NBS1 proteins (MRN complex), as well as BRCA1 to the DSB site (A, dashed arrows). These events activate ATM which occurs by autophosphorylation of Ser1981 and leads to dissociation of the ATM dimer onto two monomers that are enzymatically active. Activated ATM is then recruited to the site of the DSB (B, dashed arrow) where it phosphorylates several substrates including NBS1, BRCA1 and SMC1 (C). NBS1 phosphorylation is required for targeting ATM to phosphorylate Chk1 and Chk2. Phosphorylation of SMC1 activates S-phase checkpoints whereas BRCA1 phosphorylation engages this protein in the DSB repair pathway. ATM also phosphorylates as E2F1, Chk1, p53, Mdm2, Chk2, and H2AX and several other substrates. Activated p53 (phosphorylated on Ser 15) induces transcription of $p21^{WAF1}$ and/or Bax genes whose protein products arrest cells in $G_1$ or promote apoptosis, respectively.

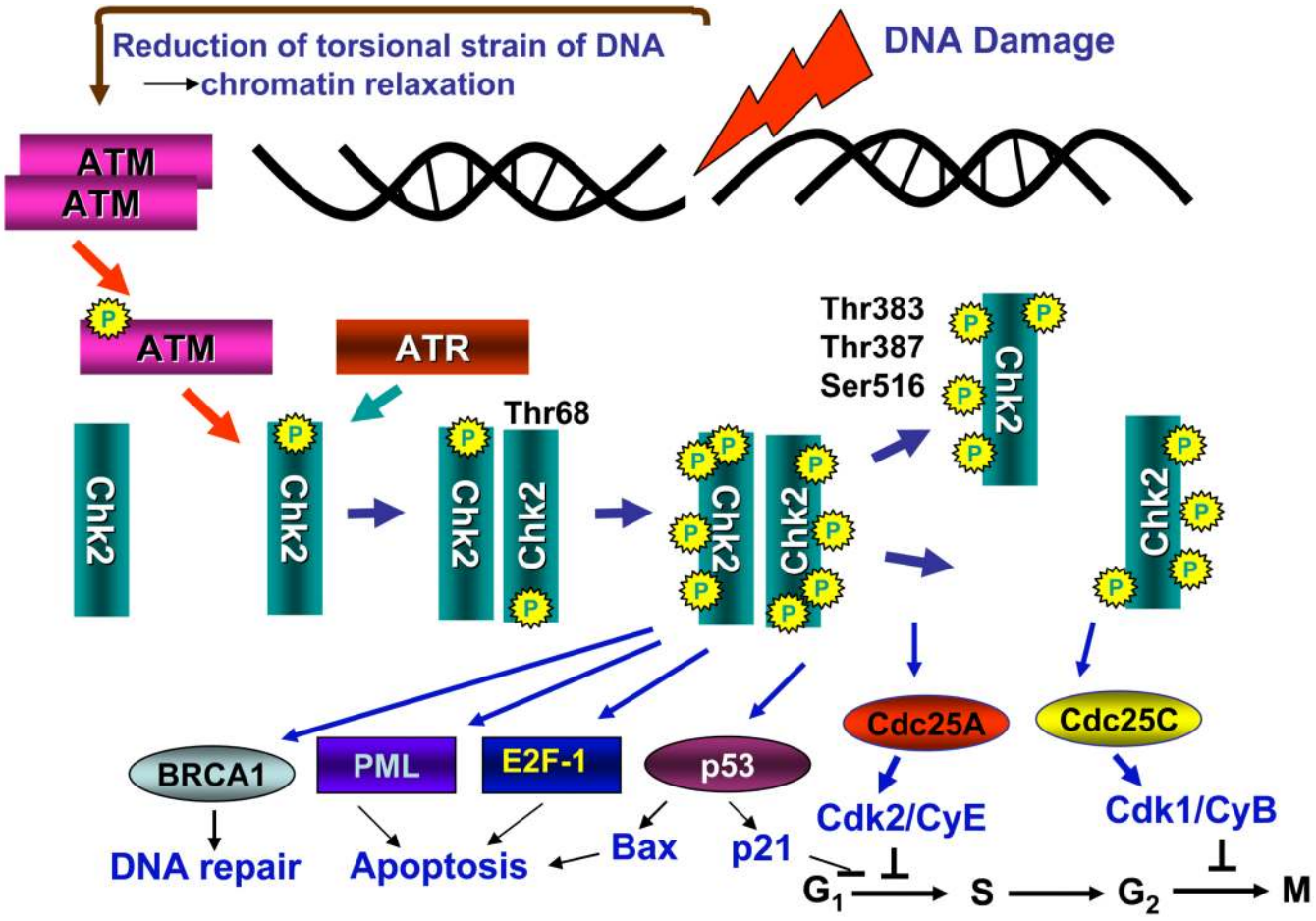


**Fig. 2. Activation of Chk2 and Chk2's major substrates**

DNA damage (induction of DSBs) triggers activation of ATM (Fig 1) which in turn phosphorylates Chk2 on *Thr*68 causing its dimerization. Phosphorylation of Chk2 can also be mediated by ATR but this occurs in response to replication stress rather than DSB. Within the dimer of Chk2 phosphorylation at *Thr*383, *Thr*387 and *Ser*516 takes place which leads to dissociation of the dimer onto monomers. Both multiphosphorylated dimers and monomers of Chk2 are enzymatically active and able to phosphorylate the downstream substrates. Among these substrates are the Cdc25C and Cdc25A phosphatases whose phosphorylation by Chk2 promotes binding to a 14-3-3 protein (Rudolph, 2007) thereby preventing translocation into the nucleus and dephosphorylation of inhibitory phospohorylations at *Thr*14 and *Tyr*15 on cyclin/CDK complexes. This halts cell cycle transitions from $G_2$ to M (Cdc25C) and $G_1$ to S, (Cdc25A) respectively. Phosphorylation of Cdc25 phosphatases also accelerates their proteasomal degradation (Boutros *et al.*, 2006). A redundant mechanism of cell arrest in $G_1$ involves phosphorylation of p53 by Chk2 which may lead to upregulation of the cdk2 inhibitor $p21^{CIP1/WAF1}$. Phosphorylation of p53 may also result in upregulation of the proapoptotic protein Bax. Apoptosis may additionally be promoted by phosphorylation of PML and E2F-1. Phosphorylation of BRCA1 engages it in the DNA repair pathway.

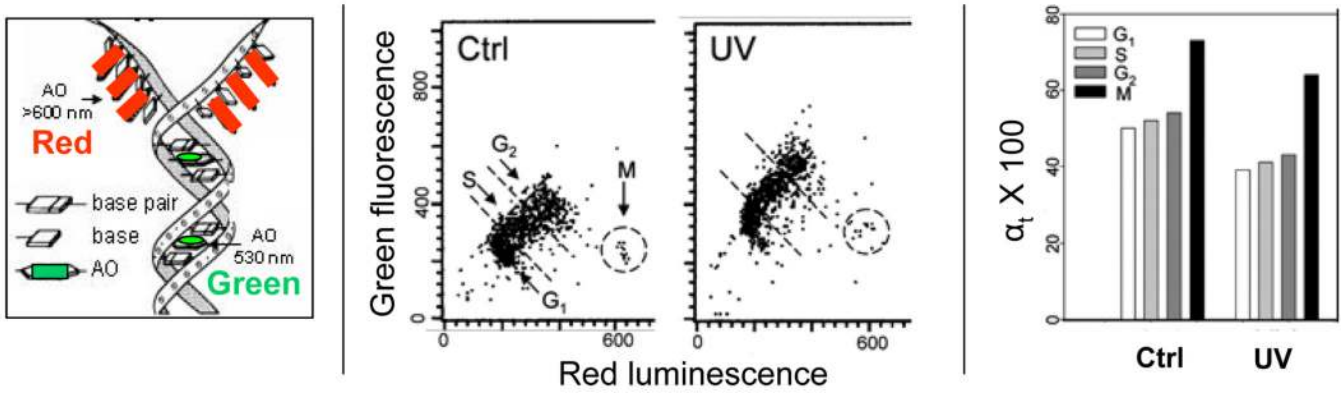


**Fig. 3. Relaxation of chromatin of TK6 cells treated with UV light detected as susceptibility of DNA to denaturation after staining with acridine orange (AO)**

The left panel shows schematically the principle of differential staining of double-stranded (ds) versus single stranded (ss, denatured) DNA sections with the metachromatic fluorochrome AO. AO binding to ssDNA results in red luminescence (>640 nm) whereas its binding to dsDNA results in green fluorescence (530 nm). (Darzynkiewicz, 1990, Darzynkiewicz and Kapuscinski, 1990, Kapuscinski and Darzynkiewicz 1984a,b). The center panels show bivariate distributions of human leukemic TK6 cells untreated (Ctrl) or exposed to 100 J/m$^2$ UV, then cultured for 30 min, fixed, treated with RNase A, subsequently with 0. 1 M HCl to induce partial DNA denaturation, and then stained with AO at pH 2.6. (Halicka et al., 2009). The extent of DNA denaturation is assessed by flow cytometry as the intensity of red luminescence (ssDNA) and green fluorescence (dsDNA). Note a decrease of red luminescence and an increase of green AO fluorescence of the UV-treated cells compared to control, reporting decondensation of chromatin. DNA in mitotic cells (M) is much more susceptible to denaturation than in interphase cells and this is reflected by their high red and low green intensity of emission (Darzynkiewicz *et al.*, 1977). The $G_1$, S, $G_2$ and M cell subpopulations thus can be identified and gated as shown by the dashed-line borders. The mean intensity of red luminescence (ssDNA) to total (red + green) intensity of emission (reporting ssDNA + dsDNA) was calculated for cells in each of these subpopulations. This DNA denaturation index (reporting approximate fraction of denatured DNA, $\alpha_t$) is plotted (as $\alpha_t \times 100$) in the right panel.

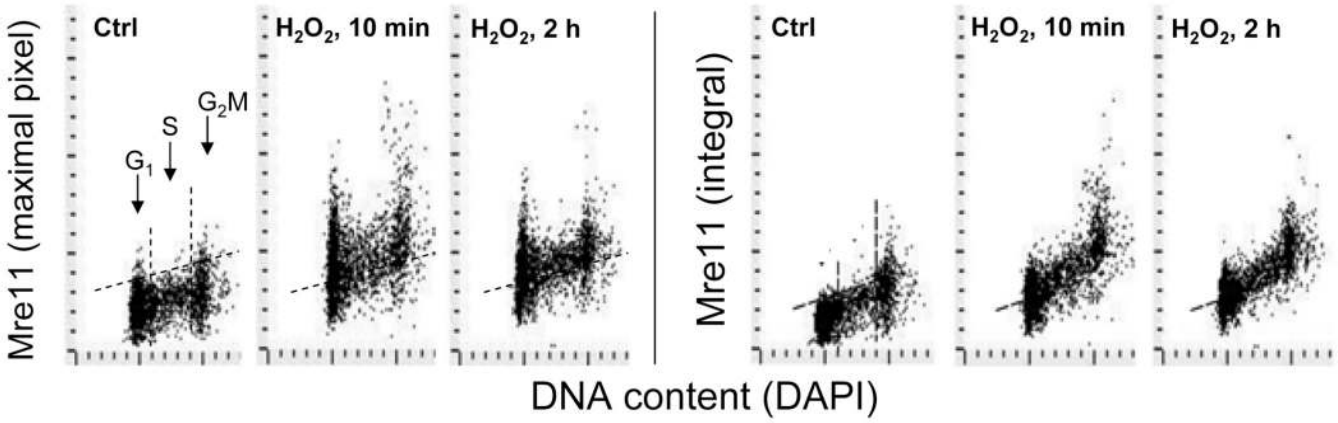


**Fig. 4. Detection of Mre11 in A549 cells treated with $H_2O_2$**

Exponentially growing cells untreated (Ctrl) or treated with 200 μM $H_2O_2$ for 10 min or 2 h were fixed and the expression of Mre11 in cell nuclei, detected immunocytochemically, was measured by LSC. Cellular DNA was counterstained with DAPI. Bivariate distributions show expression of Mre11 with respect to the cell cycle phase measured either as maximal pixel or as integrated value of Mre11 immunofluorescence (IF). The dashed skewed lines show the upper threshold level of Mre11 IF for 95% of cells in Ctrl. The maximal increase in Mre11 IF was seen during the initial 10 min followed by a decline (see Zhao *et al, 2008* for further details and kinetics data).

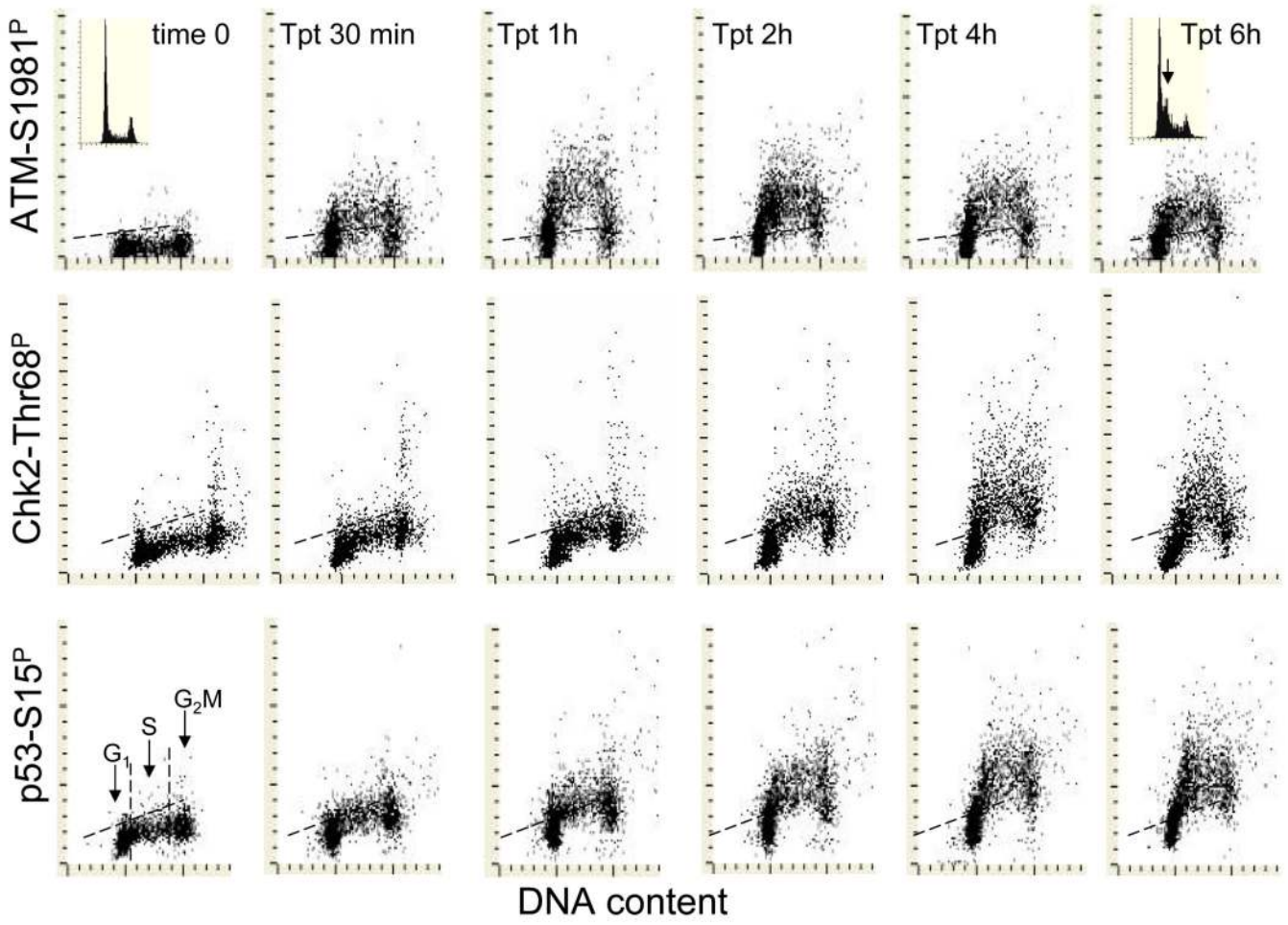


**Fig. 5. Kinetics of induction of phosphorylation of ATM on *Ser*1981, Chk2 on *Thr*68 and p53 on *Ser*15 in A549 cells treated with the DNA topoisomerase I inhibitor topotecan (Tpt)**

The bivariate distributions of DNA content versus, ATM-S1981$^P$ (top), Chk2-Thr68$^P$ (mid) and p53-S15$^P$ (bottom panels) of A549 cells treated with 150 nM Tpt for up to 6 h. Cells in $G_1$, S and $G_2$M can be identified based on differences in DNA content as marked in the control (time 0) culture. The dashed skewed lines represent the upper threshold level of IF for 97% of interphase ($G_1$ and S) cells in the respective control cultures. The insets in the DNA versus ATM-S1981$^P$ distributions show DNA content frequency histograms of cells from time 0 (left) or 6 h Tpt treated (right) cultures. Note the accumulation of cells in early S-phase (arrow) as a result of cell arrest in S by Tpt after 6 h.

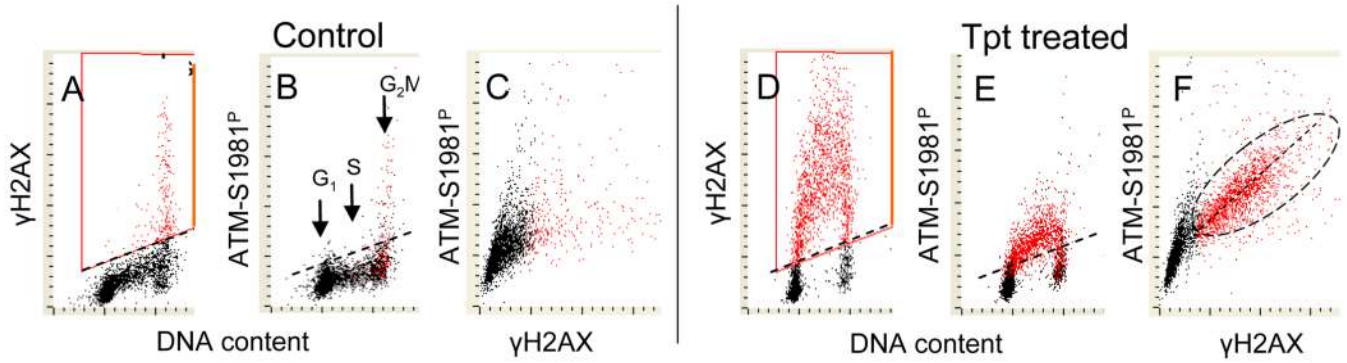


**Fig. 6. Correlation between ATM activation and H2AX phosphorylation in A549 cells treated with Tpt**

Untreated (Control; A, B,C) and Tpt-treated (150 nM, 1 h; D,E,F) A549 cells were subjected to immunostaining using phosphospecific Abs to differentially label γH2AX and ATM-S1981$^{P}$ with Alexa Fluor 488 and Alexa Fluor 670 Abs, respectively. Cellular DNA was counterstained with DAPI; the emitted blue, green, and far red fluorescence was measured using a three-laser LSC. Using "*paint-a-gate*" analysis, the cells expressing γH2AX were colored red (A, D). Note that nearly all cells with elevated expression of ATM-1981$^{P}$ (B, E) are red-colored which indicates that H2AX is phosphorylated in the same cells that have activated ATM. On the bivariate distribution of γH2AX versus ATM-S1981$^{P}$ a good correlation between intensity of expression of there phosphoproteins is seen in the Tpt – treated cells (F) (Tanaka *et al.*, 2007a). Among the untreated cells (control) only premitotic and mitotic cells constitutively express γH2AX and ATM-S1981P (Zhao *et al.*, , 2007, 2008c).

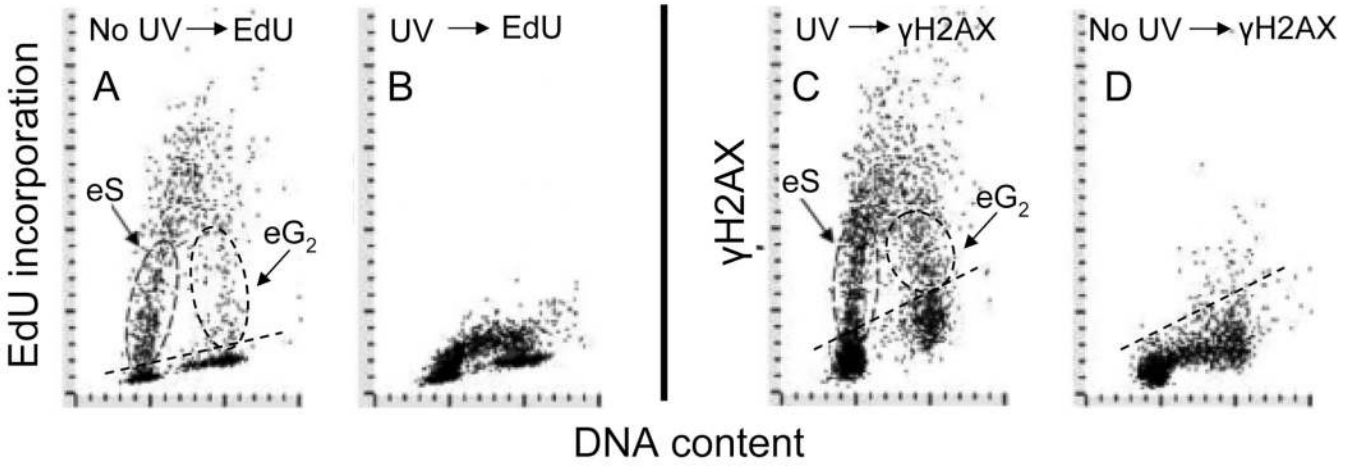


**Fig. 7. Correlation between DNA replication and phosphorylation of H2AX after exposure of cells to UV light**

Exponentially growing A549 cells, untreated (panels A and D) or exposed to 50 J/m$^2$ of UV-B light (B and C) were incubated for 60 min with 5'-ethynyl-2-deoxyuridine (EdU) then fixed. Incorporation of EdU was detected using the click chemistry approach (Salic and Mitchison, 2008; see Chapter xxxx of this volume) with AlexaFluor® 488 tagged azide ("click-iT™ imaging kit", Invitrogen/Molecular Probes, Carlsbad, CA), Expression of γH2AX was detected using Alexa Fluor 633 secondary Ab (far red fluorescence), DNA was counterstained with DAPI (Zhao *et al.*, 2019). Subpopulations of cells entering S (eS) and $G_2$ ($eG_2$) during the 60 min pulse with EdU are outlined with the dashed oval lines.

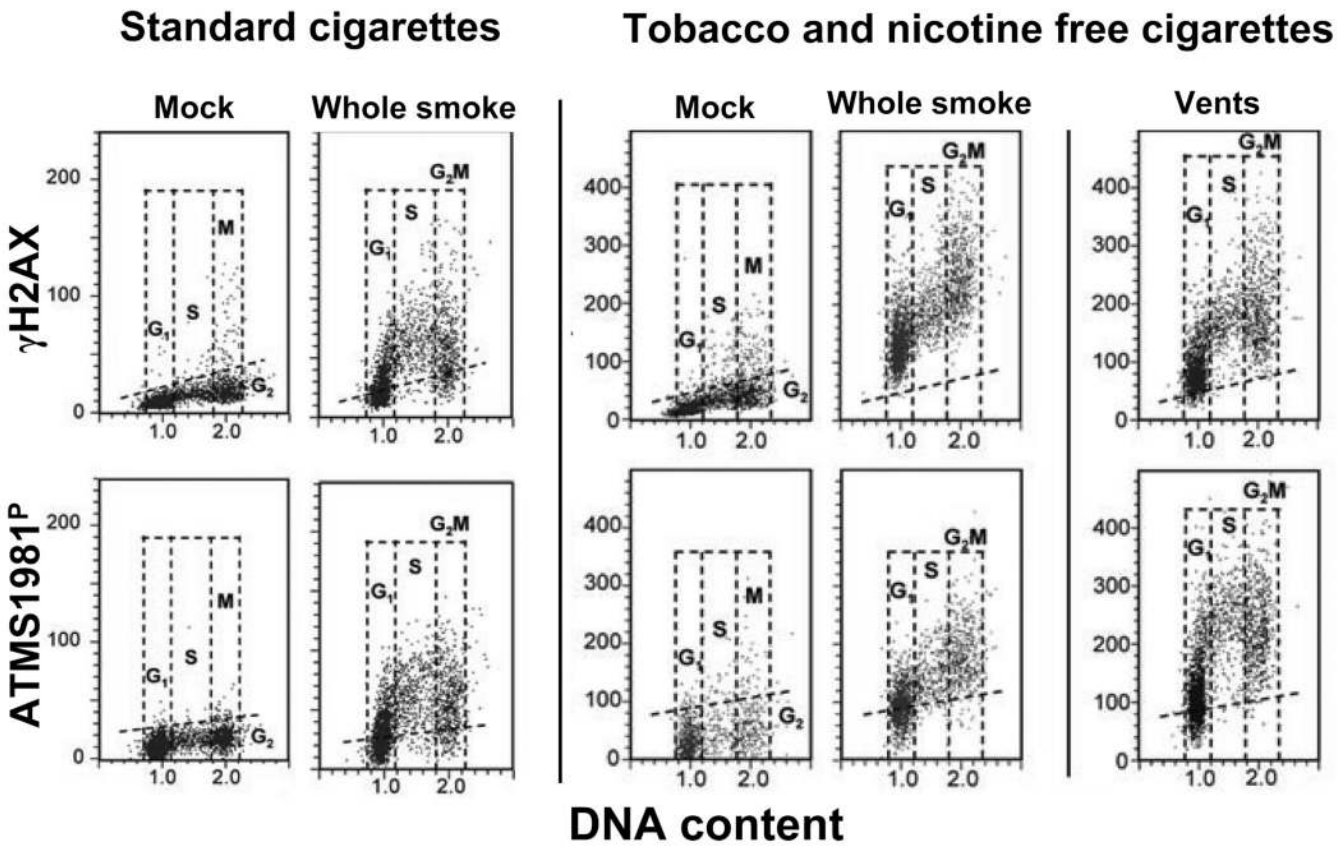


**Fig. 8. Induction of γH2AX and ATM-S1981$^P$ in A549 cells after their exposure to either standard (2R4F) cigarette smoke (CS) or to smoke from the tobacco- and nicotine-free cigarettes (T&N free)**

Cells were either mock-treated (exposed to the ambient air) or exposed to whole smoke from 2R4F (considered a standard "light cigarette) or to a T&N free cigarette for 20 min and then incubated in culture for 1 h. The right panels ("vents") shows the cells that were exposed to smoke from T&N-free cigarettes with open vents whose function is to dilute the smoke with air (Jorgensen *et al.*, 2010). The bivariate DNA content (DNA index; DI) versus γH2AX (top panels) or DNA content versus ATM-S1981$^P$ (bottom panels) distributions show the expression of γH2AX and ATM-S1981$^P$ with respect to the cell cycle phase; cells in $G_1$, S and $G_2$M phases of the cell cycle were identified based on differences in DNA content as shown . The dashed skewed lines indicate the upper threshold for γH2AX or ATM-S1981$^P$ IF for 95% of the mock-treated cells.

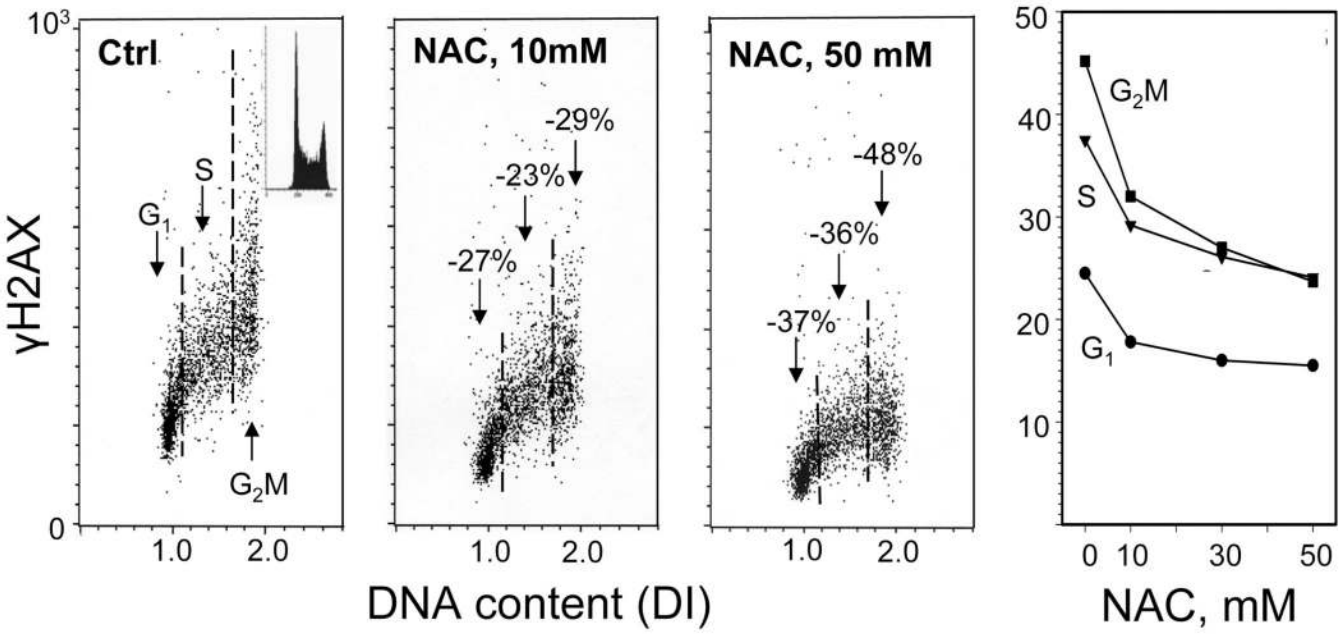


**Fig. 9. Attenuation of constitutive expression of γH2AX in TK6 cells exposed to N-acetyl-L-cysteine (NAC)**

The bivariate (DNA content versus γH2AX IF) distributions show a decrease in the level of constitutive expression of γH2AX in cells growing in the presence of 10 or 50 mM NAC, added into cultures for 1 h prior to cell harvesting compared to the untreated cells (Ctrl). The percent declines in mean values of γH2AX IF of $G_1$, S and $G_2$M phase cell subpopulations in cultures treated with NAC in relation to the respective subpopulations of the untreated (Ctrl) cells, are marked. The inset in the left panel shows the DNA content frequency histogram representative of the cells in these cultures. The right panel shows the plot of the mean values of γH2AX IF for $G_1$, S and $G_2$M cells, estimated by gating analysis, in relation to NAC concentration (Tanaka *et al.*, 2006).

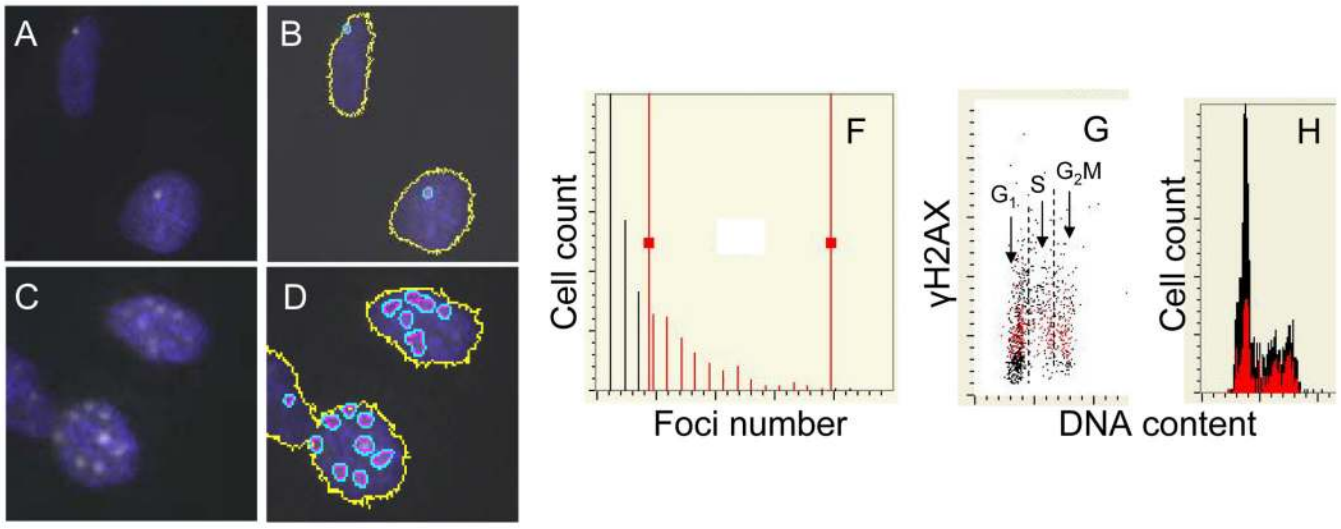


**Fig. 10. Analysis of γH2AX foci by laser scanning cytometry (LSC)**

A549 cells were either "mock-treated" (A, B) or exposed to smoke from 2R4F tobacco containing cigarettes for 8 min (C,D) and then incubated in culture for 1 h, as described in the legend to Fig. 8. After fixation the presence of γH2AX was detected immunocytochemically (Albino *et al.*, 2009,Jorgensen *et al.*, 2010). The expression of γH2AX was confined to the characteristic IF foci which were more abundant in the smoke-exposed cells. The LSC software, initially developed to quantify fluorescence *in situ* hybridization (FISH) foci (Kamentsky *et al.*, 1997) have been used to contour and count images of the γH2AX foci (B,D).The multiparameter analysis of LSC was used to plot the distribution of cells from the smoke-exposed cultures with respect to number of foci per cells (E) and the relationship between expression of γH2AX per nucleus and DNA content (F). The gating analysis was performed to select cells with greater than three foci (F, "red gate") and through "paint-a-gate" analysis to visualize these cells as colored red on the γH2AX versus DNA content bivariate distribution (F), and their cell cycle position on the DNA content histogram (G).